

# PHYSICAL AND CHEMICAL VOLCANOLOGY OF THE EOCENE MOUNT CLISBAKO VOLCANO, CENTRAL BRITISH COLUMBIA

By P. Metcalfe, T.A. Richards, M.E. Villeneuve, J.M. White and C.J. Hickson  
Geological Survey of Canada

*Geological Survey of Canada Contribution 1996160*

**KEYWORDS:** Interior Plateau, British Columbia, epithermal mineralization, clisbako, eocene, volcanic centre, calc-alkaline, potassic, pyroxene-phyric, intermediate, felsic, biotite-phyric, pyroclastic eruption, caldera, flow-domes,  $^{40}\text{Ar}/^{39}\text{Ar}$  Isotopic ages, palynology, geochemistry, trace elements, chemical models.

## INTRODUCTION

This paper summarizes current results of reconnaissance geological mapping, sampling and petrologic analysis of Tertiary volcanic rocks in the Clisbako River area of central British Columbia, carried out as part of the (1991-1995) Canada - British Columbia Agreement on Mineral Development (van der Heyden *et al.*, 1993, 1995). This work complements other studies in this area such as drift mapping (Proudfoot, 1993), a lake sediment geochemical survey (Cook, 1993, 1995) and a multiparameter geophysical survey (Shives and Carson, 1994).

A preliminary study of Tertiary volcanic stratigraphy in the Clisbako area of central British Columbia (Figure 1)

began in September 1993. The purpose was to determine the stratigraphic succession and petrologic relationships of the Early Tertiary felsic volcanic rocks which host epithermal mineralization discovered on the Baez and Clisbako claim groups (MINFILE 093C 015 and 093C 016, respectively), near the headwaters of the Clisbako River. Results are compared with information from Tertiary volcanic rocks exposed to the north in the Nechako River area (93F; Green and Diakow, 1993; Diakow *et al.*, 1993; Diakow and Webster, 1994) and to the south in the Taseko Lakes area (92O; Hickson *et al.*, 1991; Hickson, 1992, 1993; Hickson and Higman, 1993).

The study area is part of the Chilcotin Plateau and comprises four 1:50 000 map sheets (93B/12, B/13, C/9, C/16), bounded by latitudes 52°30"N and 53°00"N and by longitudes 123°30"W and 124°30"W (Figure 2). Relief is gentle and the area is forested. Outcrop is not abundant. The area is accessible by means of numerous logging roads, west from Quesnel and northwest from Alexis Creek.

## GEOLOGY OF THE CLISBAKO AREA

The pre-Eocene basement rocks in the Clisbako area are exposed as discrete inliers, usually as ancient ridges, more resistant to erosion than the younger rocks which overlie them (Figure 2). The Eocene volcanic rocks are the focus of the present study and therefore only a few outcrops exposing the older assemblages were visited during the course of fieldwork.

### FOSSILLIFEROUS LIMESTONE (TRIASSIC)

This unit is exposed in only one location in the study area, which was not visited. Tipper (1959) described a small area in the McFarland Creek valley underlain by rocks which he tentatively identified as Cache Creek Group. The unit is exposed over a larger area than originally described and forms a low ridge, surrounded by the younger Eocene and Chilcotin lavas (Figure 2). Tipper (personal communication, 1996) described the unit as a grey-weathering fossiliferous limestone of Triassic age, based on paleontological evidence.

### JURASSIC VOLCANIC AND SEDIMENTARY ROCKS

Two parts of the study area are underlain by an assemblage of intermediate fragmental rocks. Tipper (1959;

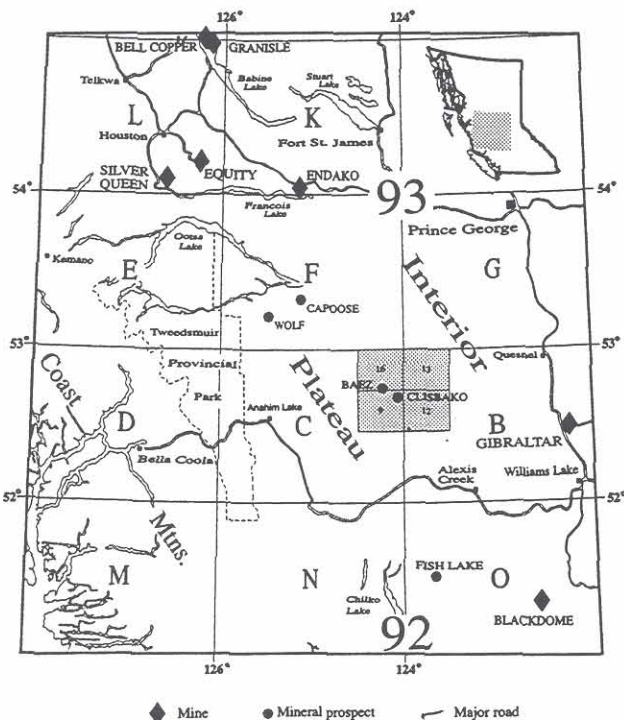


Figure 1. Location of the study area.

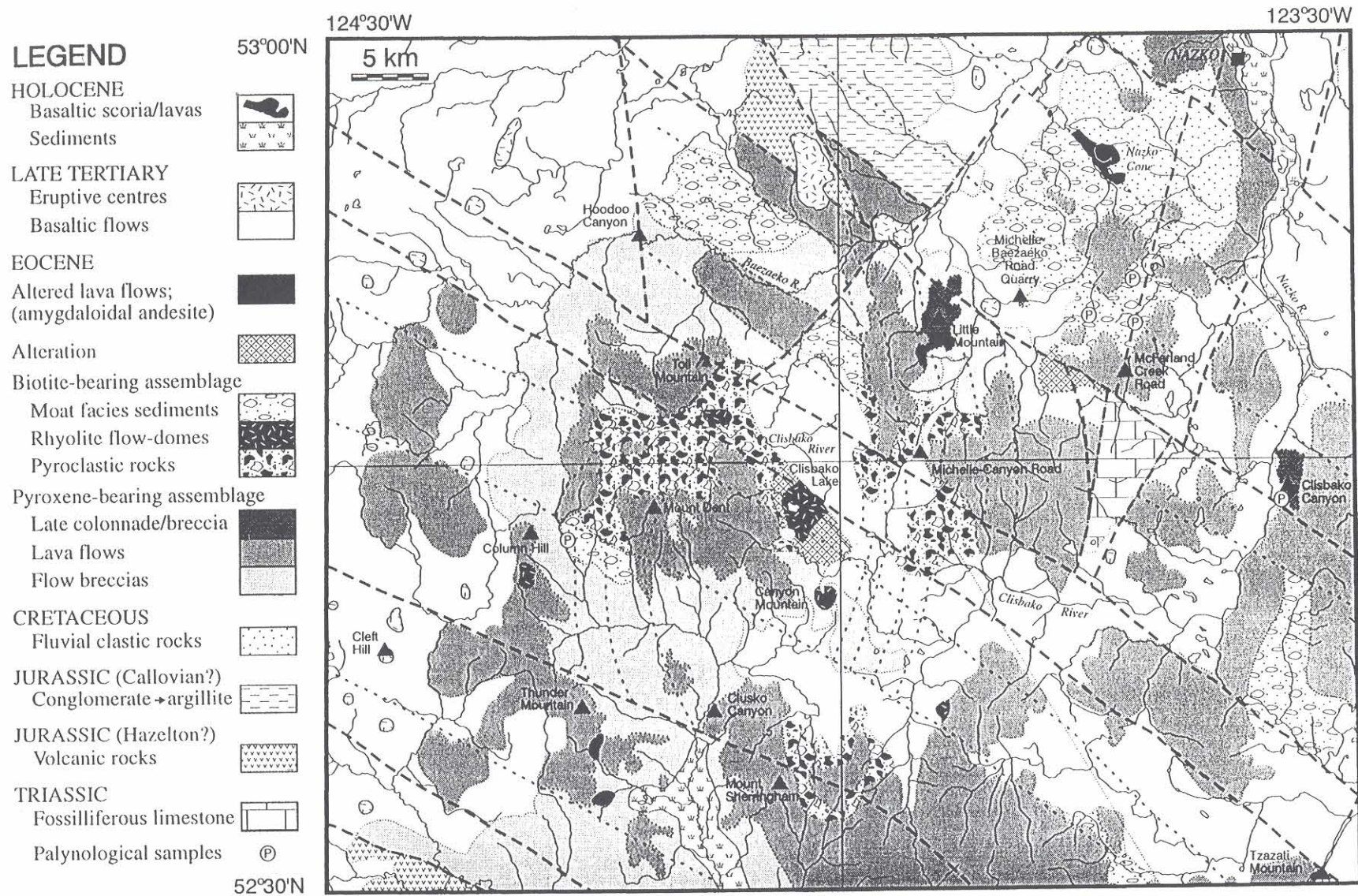
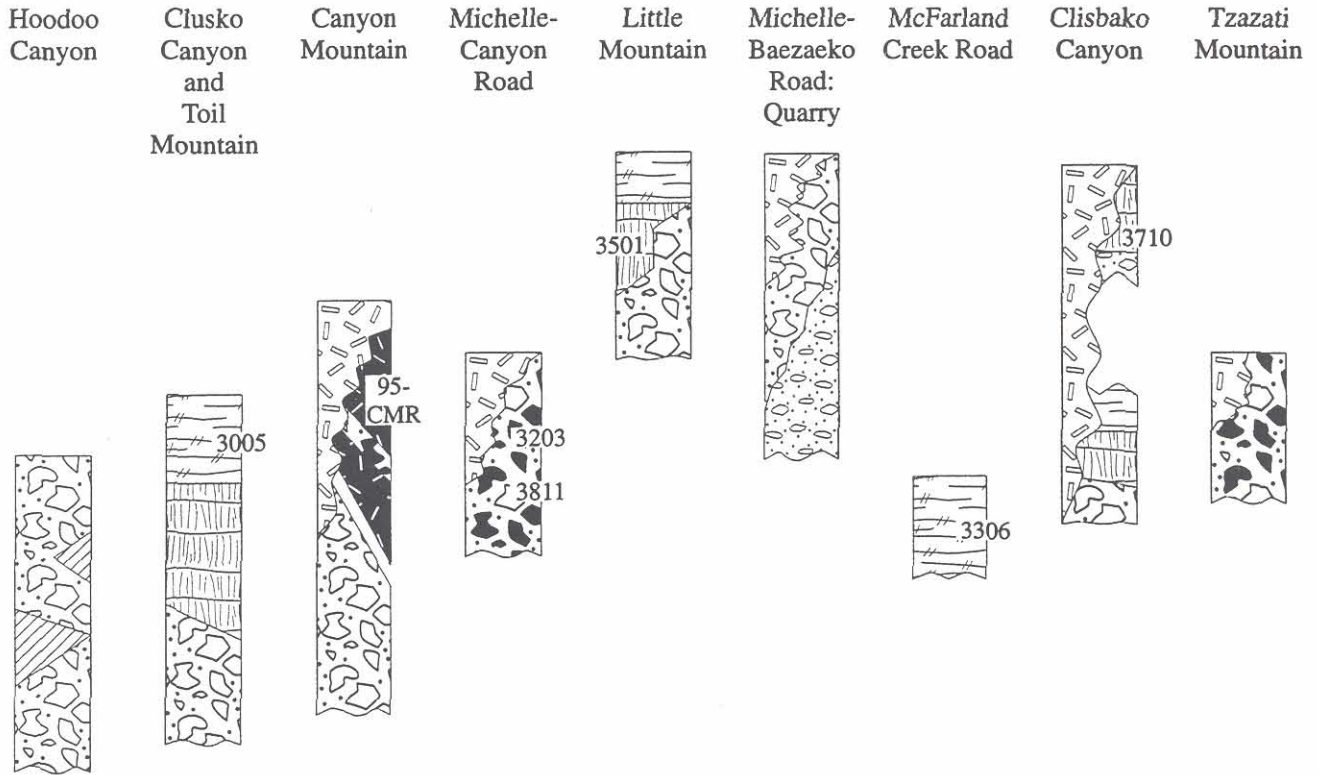


Figure 2. Geological map of the Clisbako area (this study; Tipper, 1959, 1969; Richards and others, unpublished data). Eocene volcanic rocks rest on a deformed basement of presumed Mesozoic age and are partially covered by valley-filling Chilcotin Group basalts. The area was glaciated and outcrop is not abundant. Probable and possible faults (heavy and light dashed lines) are inferred from juxtaposition of rock units, magnetic discontinuities (G.S.C., 1994) and topographic lows.



**CHILCOTIN GROUP (MIOCENE)**

 Plagioclase-olivine phyric basalts, overlying Eocene volcanic rocks with erosional unconformity and filling paleovalleys

**CLISBAKO VOLCANICS (EOCENE)**

**Plagioclase+augite-bearing assemblage**

 Pyroxene and/or plagioclase-phyric dacite flows, often flow laminated or flow banded and as much as 100 m thick.

 Plagioclase-phyric dacite columnades, grading laterally/down section to flow-breccia. Variable thickness, as much as 100 m.

 Flow breccias with pyroxene-bearing dacite boulders and rare coherent flow lobes. Some units may be related to biotite-bearing moat facies.

**Biotite-bearing assemblage**

 Moat facies; biotite-bearing clastic sedimentary or epiclastic rocks containing plant remains. This facies may include dacite flow breccias.

 Biotite-bearing pyroclastic/epiclastic rocks, containing blocks of biotite rhyolite and accidental blocks of pyroxene-bearing dacite.

 Biotite, quartz and feldspar-phyric rhyolite flow domes, intercalated with or grading laterally into flow breccias.

Figure 3. Stratigraphic sections through Eocene volcanic assemblages in the study area; locations of sections are shown on Figure 2. Samples analysed for <sup>40</sup>Ar/<sup>39</sup>Ar are shown by number. The biotite-bearing assemblage is recessive, but includes a large number of accidental fragments of pyroxene-phyric dacite. In some sections it is overlain by dacite columnades which are clearly younger. The biotite rhyolites are interpreted as the product of a large pyroclastic eruption, or eruptions which interrupted a long (>6 Ma) period of dacitic volcanism.

1969) assigned this assemblage to the Lower Jurassic Hazelton Group, based on lithological similarity. These rocks differ from the more recent volcanic rocks (Eocene and younger) in containing a schistose foliation. This foliation is regional only in a north-south belt, approximately 10 kilometres wide, which can be traced from the Baezaeko River northward. To the west of this belt the older rocks (Mesozoic) do not contain this strong foliation.

Scarcity of outcrop precluded comprehensive structural mapping. The limited number of outcrops examined are volcanogenic and fragmental. The rocks are brown or green, weathering to green or maroon. Lithologies vary from lapilli tuff to volcanic breccia (Fisher, 1961) and angularity varies from angular to subangular, less commonly to subrounded. The rocks include both heterolithic and homolithic types.

Fragments are most commonly weakly feldspar phyric, containing as much as 10% subhedral feldspar phenocrysts, usually less than 1 millimetre in length. Other fragments are aphanitic, some possibly with relict pumiceous texture. They are commonly matrix supported in a dark green or purple aphanitic matrix.

Immediately to the north of the Baezaeko River, at the northern edge of the study area, the Mesozoic strata comprise argillite, chert-pebble conglomerate and sandstone, all strongly cleaved. These rocks do not show the same pervasive foliation and are interpreted as possibly Callovian in age. This foliation is present only in a zone 10 kilometres-wide which can be traced northward from the study area; west of this zone the Mesozoic rocks are not cleaved (Richards and others, unpublished data).

### CLASTIC SEDIMENTARY ROCKS (CRETACEOUS)

Small, discrete exposures of clastic sedimentary rock are exposed at several locations in the northeast of the study area, towards the Nazko River valley. This poorly exposed assemblage comprises dark grey to brown argillite and lithic sandstone; Tipper (1959) and Hunt (1992) recorded conglomerate, not observed in this study. These conglomerates were intersected by exploration diamond drilling carried out on the Bob claims. The sedimentary rocks observed are thickly laminated to thinly bedded. Scarcity of outcrop precluded detailed mapping, but the rocks lack the distinctive foliation of the older volcanic rocks to the west. Tipper (1959) assigned these to the Cretaceous on the basis of lithological similarity to equivalent rocks. Hunt (1992) obtained palynological data giving ages ranging from Albian to Maastrichtian for Cretaceous sedimentary rocks in the Clisbako area.

### EOCENE CLISBAKO VOLCANICS

The Mesozoic basement rocks are overlain by a succession of intermediate to felsic volcanic rocks which are the subject of the present study (Figure 2). The Eocene

rocks underlie all higher ground in the study area and were identified by Tipper (1959, 1969) as part of the Ootsa Lake Group. The outcrop area is elevated, roughly circular, identifiable from satellite imagery and measures approximately 50 kilometres in diameter. To the north, the Eocene strata abut against a paleotopographic ridge underlain by the older volcanic rocks. Eastward, the Eocene outcrop area becomes progressively more dissected towards the valley of the Nazko River, where erosional level extends below the Eocene paleotopography. To the west and south the contacts are more abrupt, in both cases with the younger olivine-bearing basaltic lavas of the Chilcotin Group, which fill paleotopographic lows.

Hydraulic brecciation, epithermal alteration and mineralization are locally abundant in this assemblage. For this reason, the Eocene felsic and intermediate volcanic units outcropping in the study area are assigned a moderate to high exploration potential. The Eocene volcanic rocks comprise three lithologic assemblages, identified on the basis of fieldwork and petrography. Contacts between the assemblages are not exposed and stratigraphic relationships are inferred from the relative positions of the assemblages and, where available, their  $^{40}\text{Ar}/^{39}\text{Ar}$  isotopic ages. Relationships observed at nine sections in the study area are shown in Figure 3.

### PYROXENE-BEARING ASSEMBLAGE

The most commonly exposed assemblage comprises weakly to moderately porphyritic intermediate lavas and related breccias, containing plagioclase and/or pyroxene phenocrysts. The preliminary name "augite-bearing assemblage" (Metcalf and Hickson, 1994, 1995) is here replaced by "pyroxene-bearing assemblage" after the discovery of



Photo 1. Dacite flow-breccia, showing black glassy appearance of fresh dacite and brown to white weathering surfaces. The largest block exhibits flow banding while the black glassy block at upper left has a perlitic texture.

small but significant numbers of orthopyroxene phenocrysts in many of the samples.

Phenocrysts are usually less than 3 millimetres in length and comprise, at most, 15% of the rock. The groundmass is distinctive, being black and glassy in the freshest specimens and dark grey, weathering to cream or brown, in devitrified or slightly altered samples (Photo 1). The glassy or aphanitic nature of the groundmass distinguishes this suite of rocks from the overlying Chilcotin Group basaltic lavas.

The part of the pyroxene-bearing assemblage inferred to be the lowest stratigraphic unit is exposed mainly in the west of the study area (Figure 2). The basal, or distal, units form a thick sequence of flow breccias, containing glassy aphanitic, aphyric and plagioclase and plagioclase-pyroxene-phyric blocks, as much as 2 metres across, in a red, yellow or cream-weathering matrix. The flow breccias are intercalated with discontinuous lobes of coherent dacite, interpreted as unbrecciated flow lobes within the breccia on the basis of near-identical textures and chemical com-

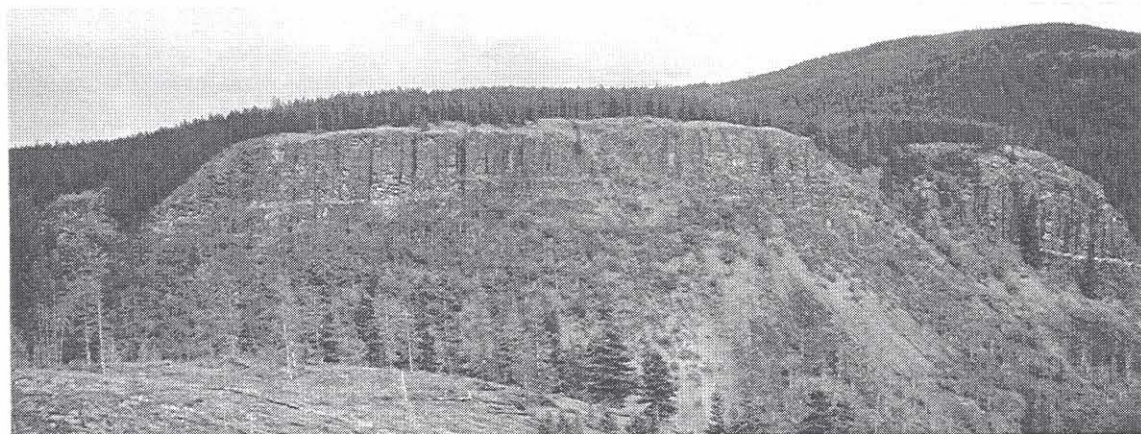


Photo 2. Section of the pyroxene-bearing assemblage exposed in Clusko Canyon. A dacite colonnade overlies and passes laterally into equivalent flow breccias and is overlain by flow-laminated dacite of identical composition, probably a zoned flow.



Photo 3. Radiating colonnade in later dacite flow dome at Column Hill, in the west of the area.

positions. Both blocks and lobes commonly contain spectacular examples of flow banding, flow folding and perlitic cracking.

Areas underlain by the flow breccias have moderate topography; outcrop is sparse and usually occurs near contacts with the more resistant overlying units, which form a protective cap (Photo 2). The flow-breccia sequence is at least 100 metres in total thickness and is probably repeated many times; isotopic data for this assemblage are too few to construct a detailed stratigraphic sequence.

The flow-breccia units pass laterally into and are overlain by black glassy flows very similar in lithology to the blocks and flow lobes in the breccias. These flows are mainly dacitic, although their distribution in the field suggests a more fluid and mafic composition (Metcalf and Hickson, 1994). The dacites contain between trace and 15% plagioclase, with or without pyroxene phenocrysts. They are interpreted as proximal, unbrecciated equivalents of the flow breccias.

The lava flows locally exhibit flow banding and flow folding. Many may be dry flow domes, as the flow foliation is commonly steep. This lithology is resistant to erosion and forms rare cliff exposures with spectacular colonnades as much as 30 metres high. The total thickness of this part of the succession could not be measured, due to lack of continuous outcrop; it probably varies greatly throughout the area. Significant exposures occur at Little Mountain, Clisbako Canyon, Clusko Canyon, Thunder Mountain and 8 kilometres west of Mount Dent, at Column Hill (Figure

2, Photo 3). In the central part of the area, near Clisbako Lake, the flows grade up-section from relatively high pyroxene-plagioclase phenocryst contents to weakly pyroxene-phyric flows.

Exposures of colonnade-forming lavas are overlain by strongly flow-laminated lavas. These lavas are also mainly of dacitic composition. The rocks are weakly vesicular; the vesicles are usually less than 2 millimetres in diameter and irregular in shape. Flow banding is rare; instead, flow layers (Photo 4) are defined by smearing of vesicles in planes parallel to the basal contact. This fabric is deformed in some lava flows to form flow folds. In some locations, such as Clusko Canyon, the upward transition from colonnade to flow-laminated lava, partially exposed on a cliff face (Photo 2) appears to be part of the flow morphology. Certainly the chemical compositions of the colonnade and flow-laminated lava are closely similar. In this location and in several others, flow-laminated lava may represent the upper part of thick (100 metres) dacite flows, while the colonnades represent parts of the flow base and centre.

Elsewhere, flow-laminated dacite occurs as discrete flows or as lobes within the volcanic breccias. Several ridges, particularly near the periphery of the Eocene outcrop area, are cored or capped by flow-laminated lavas, possibly lateral equivalents of the colonnade-forming flows. No flow tops were observed in the course of the present study.

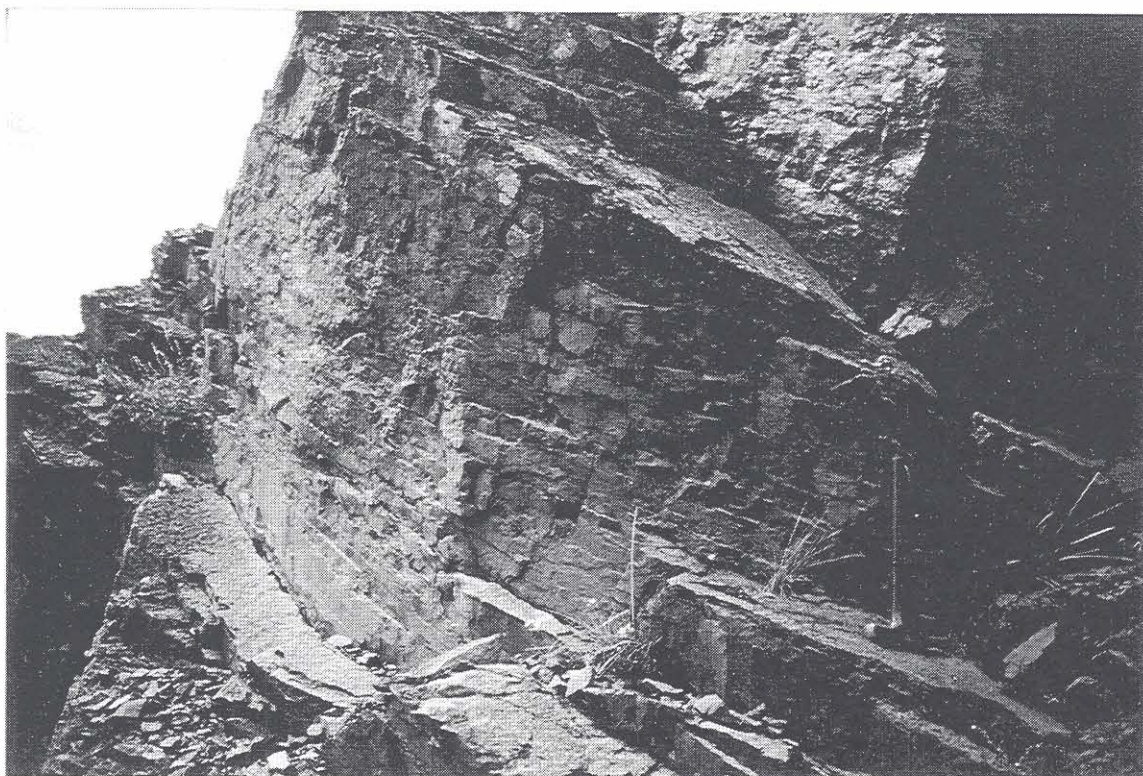


Photo 4. Flow laminations near top of exposure at Clusko Canyon (Photo 2). The laminae are probably formed by streaking out of vesicles in viscous lava, in a manner analogous to the development of "platy" colonnades in basalt.

## BIOTITE-BEARING ASSEMBLAGE

The second assemblage exposed in the study area is identified by the presence of abundant phenocrysts of primary biotite, in addition to plagioclase and, less commonly, hornblende. Lavas of this assemblage are typically rhyolitic. Fresh surfaces are light grey in colour with a characteristic greasy vitreous lustre, in which subhedral to euhedral phenocrysts of the diagnostic biotite are easily visible. The lava weathers to a dull grey or brownish grey; where altered, weathered surfaces are white to cream. Locally, flow breccias may occur, grading laterally into flows (Photo 5).

The rhyolitic lavas are restricted to small flow domes near the centre of the area. At least four such eruptive centres are located, on a roughly northwest trend, in the central and west-central part of the area. Typical of these is Canyon Mountain (Figures 2 and 3). This distinctive mountain comprises a flow-dome complex (Photo 6) consisting of biotite-porphyrific rhyolite flows and flow breccias intercalated with pyroclastic and epiclastic fragmental units of similar composition (Photo 7). Southwest of Canyon Mountain is a 10 metres-wide porphyry dike of quartz-hornblende-feldspar and a second knoll of hornblende-biotite-quartz phyrific rhyolite, also interpreted as a flow dome. To the northwest of Clisbako Lake, on the south side of the Clisbako River valley, is a brecciated and



Photo 5. Homolithic flow-breccia, grading laterally into biotite rhyolite lava in the flow-dome at Canyon Mountain.

flow-banded biotite-quartz-phyric rhyolite, with broken quartz phenocrysts, interpreted as an autobrecciated flow-dome.

South of Clisbako Lake are small exposures of a white to buff-weathering felsic rock; contacts are obscured at all localities examined. The unit may therefore be intrusive or extrusive in origin, but studies of the unit T.A. Richards and others, unpublished data noted abundant broken crystals and a lack of flow textures, suggestive of a pyroclastic origin. The unaltered rock contains subhedral biotite phenocrysts (1-2 mm) and 20-25% euhedral to subhedral quartz phenocrysts (2-5 mm) in an extremely fine grained groundmass. This abundance of modal quartz is unusual in the Eocene volcanic rocks. Quartz phenocrysts enclose relict biotite and the occurrence of altered biotite phenocrysts indicates that the unit is part of the biotite-bearing assemblage. Minor hornblende phenocrysts are also present. Quartz porphyries are exposed in several localities throughout the area, often close to mineralization, including that discovered at Clisbako and also on the Bob mineral claims in the northeast of the area (T.A. Richards and others, unpublished data). As noted above, quartz phenocrysts are ubiquitous in this biotite-bearing assemblage. The quartz porphyries appear to postdate most, if not all the other biotite-bearing volcanic rocks and overlie lacustrine sedimentary rocks of the moat facies, described below.

A more widespread biotite-bearing lithology comprises massive breccias, lapilli tuffs and tuff-breccias (Photo 8), intercalated with volcanic sedimentary rocks. The massive units include blocks and lapilli of rhyolite, very similar in composition to the lavas, matrix supported in an altered tuff. All units observed in outcrop are heterolithic and contain lapilli and blocks of pyroxene-bearing dacite. Phenocrysts comprise biotite, hornblende and feldspar; broken crystals are abundant. This part of the assemblage is interpreted as the product of pyroclastic flows.

The pyroclastic units are very poorly lithified and weather recessively. On the lower slopes of Toil Mountain are exposures of a thick (50 m) massively bedded unit identified as a welded heterolithic pyroclastic deposit containing abundant blocks of pyroxene-bearing and aphyric dacite, fiammé, and crystals of biotite, plagioclase and quartz in a vitrophyric groundmass. Similar fragmental units crop out 11 kilometres northeast of Canyon Mountain, south of the Michelle-Canyon road (Figures 2 and 3). Here they exhibit well developed reverse grading, interpreted as the result of pyroclastic flow. Here and at Canyon Mountain, the fragmental units include blocks of plagioclase-pyroxene-phyric dacite.

Stratigraphic relations between the biotite-bearing and pyroxene-bearing assemblages are poorly known. Blocks of pyroxene-bearing dacite occur in the biotite-bearing fragmental rocks. However, northeast of Canyon Mountain, in a quarry near the junction of the Michelle-Canyon and Michelle-Baezaeko forest service roads (Figures 2 and



Photo 6. Dissected flow dome of biotite rhyolite on the west side of Canyon Mountain in the centre of the Clisbako area. The flow dome comprises lava flows and related flow breccias, intercalated with pyroclastic flow deposits.

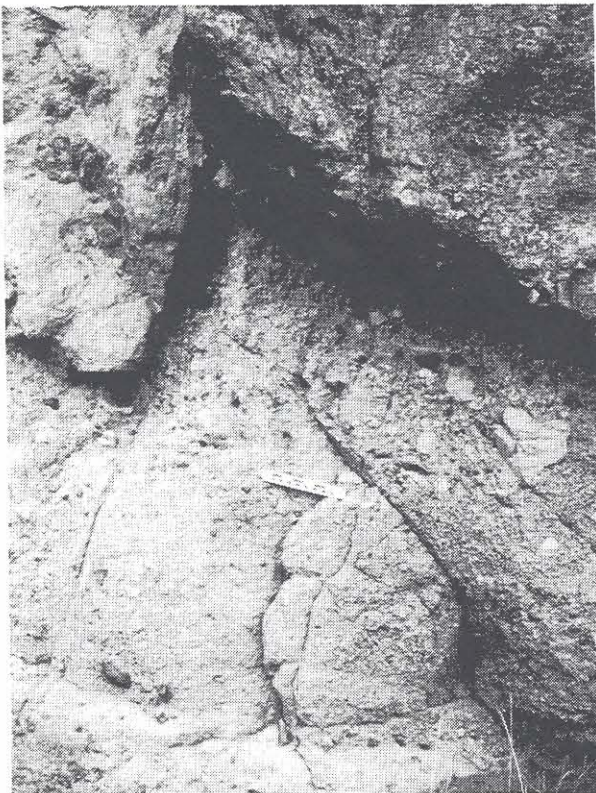


Photo 7. Pyroclastic tuff-breccia intercalated with lava flows in the flow dome at Canyon Mountain. Note the presence of blocks of biotite rhyolite (white) and accidental blocks of pyroxene-bearing dacite (black).

3), pyroxene-bearing dacite flow breccias overlie at least one unit of tuffaceous conglomerates associated with the biotite-bearing volcanic rocks. In the Michelle-Canyon roadside exposure east of Canyon Mountain (Figures 2 and 3), the biotite-bearing pyroclastic strata dip moderately to the east, apparently beneath dacite flows and flow breccias. The biotite-bearing fragmental rocks therefore occupy paleotopographic depressions in the older pyroxene-bearing volcanic products and are overlain by younger pyroxene-bearing lavas.

The biotite-bearing assemblage was noted at two other locations, one of which is on Tzazati Mountain, in the extreme southeast of the area. The outcrop is separated from those in the centre of the area by a topographic low, interpreted here as having formed by erosion of the less resistant fragmental rocks and subsequently filled with basalts of the younger Chilcotin Group. A well, drilled by Canadian Hunter Ltd. in this depression during the course of hydrocarbon exploration, intersected the base of the Chilcotin Group lavas at a depth of approximately 230 metres and the base of the Eocene volcanic sequence at approximately 600 metres. A synopsis of the drill log (Chilcotin B-22-K well) is given by Hunt (1992). At 542 metres depth, the hole intersected a horizon of white felsic rock with hornblende crystals, biotite and quartz. This is almost certainly an intersection of the biotite-bearing assemblage capped by later lava flows, including basalts of

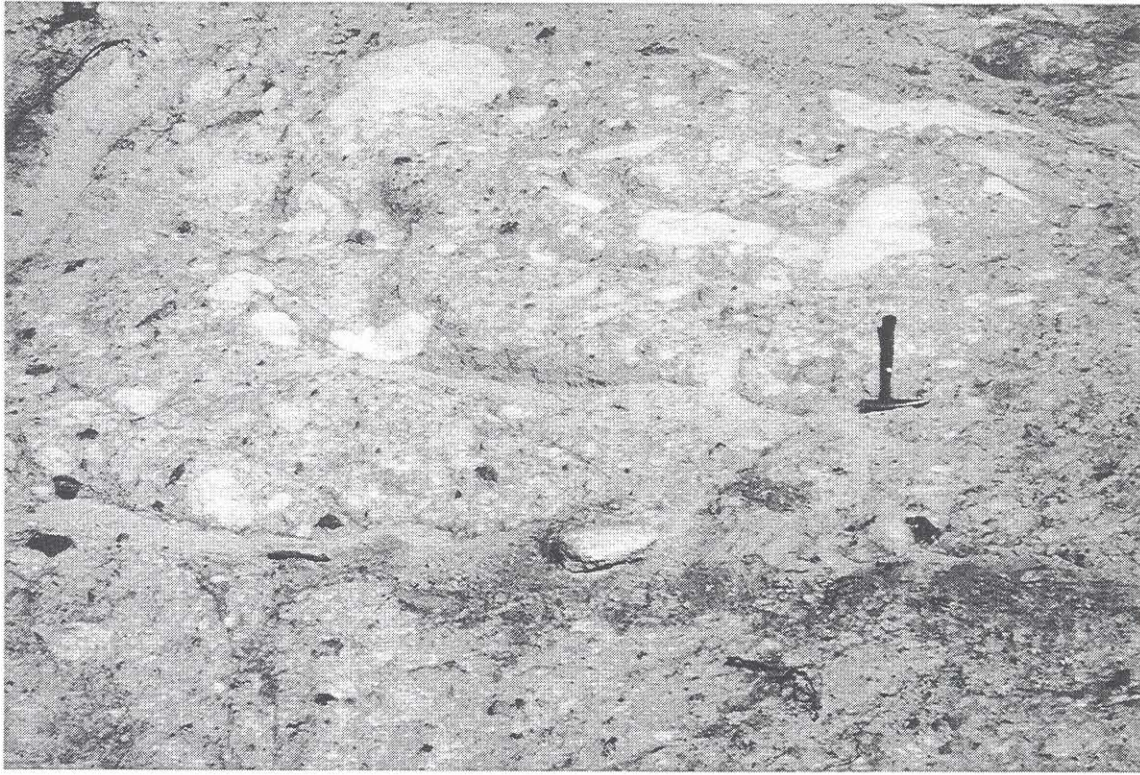


Photo 8. Pyroclastic tuff-breccia exposed near the centre of the Clisbako area. Clasts of quartz-feldspar-biotite-phyric rhyolite are subangular to subrounded and matrix supported. Accidental clasts include plagioclase-augite dacite.

the Chilcotin Group. It is apparent from the log that, in addition to the Chilcotin Group lavas, a considerable thickness of Eocene dacite lava overlies the biotite-bearing unit.

### **MOAT FACIES OF THE BIOTITE-BEARING ASSEMBLAGE**

Epiclastic sedimentary rocks are exposed in several locations in the central part of the study area. They are as poorly consolidated as the pyroclastic rocks, invariably white to bleached in colour and are extremely recessive; exposure is almost entirely man-made disturbances (roads and logging slashes).

The rocks are thickly laminated to thinly bedded and commonly show normal grading, bed perturbation and rip-up clasts, characteristic of a high-energy environment. The facies includes a wide variety of rock units and includes chaotic breccia, lahar-fanglomerate, conglomerate, poorly to well sorted lithic sandstone, laminated siltstone, claystone and minor gritty argillite; this last is locally highly carbonaceous.

The clastic sedimentary rocks are polymictic and are dominated by white, clay (kaolinite) altered lithic clasts of rhyolite with phenocrysts of biotite, quartz and feldspar; also subordinate (20-40%) clasts of unaltered, massive to flow-banded rhyolite and dacite. Fresh, unaltered biotite, quartz and feldspar crystals, with numerous angular grains of volcanic glass, occur as detritus in members that range

in grain size from boulder conglomerate/lahar to fine sandstones. These unaltered detrital mineral clasts serve to correlate the lahar/breccia members with the fine-grained, finely laminated lacustrine members of the same facies. The detrital biotite, quartz and feldspar appear identical to the phenocrysts in the biotite-bearing assemblage

The facies is distributed in a number of areas peripheral to the main area of outcrop of the biotite-bearing assemblage and is included in it partly because of this spatial association. More importantly, the facies contains detrital biotite which is absent in the rare epiclastic deposits associated with the pyroxene-bearing assemblage. The biotite-bearing sedimentary rocks are therefore interpreted to have formed as a moat facies in a topographic depression, possibly a caldera, during a period of volcanic quiescence. The disjointed occurrence of this facies is interpreted as indicating the presence of separate depositional basins, peripheral to a central rhyolite complex.

In a number of locations, particularly southeast of Fishpot Lake, the moat facies includes beds of siliceous sinter deposits, associated with the lacustrine members and suggesting deposition from a paleogeothermal spring into a lake. This is interpreted as further evidence for the existence of a major volcanic centre and suggests an age for the Eocene epithermal mineralization; all the known occurrences of widespread epithermal alteration and associated quartz and precious metal mineralization in the area are

associated with the biotite-bearing assemblage. Local hydrothermal bleaching of the younger dacites spatially associated with the biotite-bearing assemblage suggests that the hydrothermal alteration that affected the older facies was still active, but weaker during their eruption.

The chemical sedimentary and fine-grained clastic rocks contain locally abundant plant fossils, described below and, less commonly, fossil fish, which have not been studied in detail. This indicates the existence of an environment in which immature clastic and chemical sediments accumulated and supported plant and animal life during the period of volcanic activity.

### AMYGDALOIDAL LAVA

Minor exposures of amygdaloidal lava occur south of Thunder Mountain, east of Clisbako Canyon and in several other parts of the study area. These were not examined in detail nor subjected to chemical or isotopic analysis because of ubiquitous alteration. The lavas are green as a result of pervasive chlorite-epidote alteration and contain as much as 10% amygdules, 0.5 to 3 centimetres across. The amygdules contain fine-grained silica and, rarely, carbonate. The flows appear to overlie the other Eocene lithologies in the Clisbako area and probably represent the latest stages of volcanic activity in this period. No evidence of epithermal-style mineralization associated with these flows was observed during the course of fieldwork.

### <sup>40</sup>AR/<sup>39</sup>AR ISOTOPIC AGE DETERMINATIONS

Four samples from the pyroxene-bearing assemblage and three samples from the biotite-bearing assemblage were analysed for argon isotopic composition, to determine their age. The analyses were carried out at the Geological Survey of Canada's isotope laboratory in Ottawa. Due to the fresh nature of the samples and the absence of potassium-bearing phases in the dacites, a whole-rock fraction was analysed for each of the pyroxene-bearing samples. Biotite fractions from the three biotite-bearing samples were used to make the determinations, owing to the ubiquity of fresh phenocrysts of this mineral.

Analytical procedures for all samples in the pyroxene-bearing assemblage and for 95-CMR, from the flow dome at Canyon Mountain, follows that outlined in Appendix 1 of Roddick (1990). Whole-rock samples weighing 32 to 34 milligrams were loaded into aluminum foil packets, arranged in an aluminum can 40 by 19 millimetres, together with evenly distributed packets of FCT-3 biotite as flux monitors. The can was sent to the research reactor at McMaster University for 8-hour neutron irradiation in an approximate fast neutron fluence of  $3 \times 10^{16}$  neutrons/square centimetre. An age of  $27.68 \pm 0.03$  Ma was ascribed to FCT-3 (M.J. Kunk, personal communication, as quoted in Roddick, 1990) resulting in a calculated J factor of 0.00185 to 0.00187, although variation along the can, as measured with FCT-3, allowed interpolation of J

factor for samples that fell between monitors. Analytical procedure for 95-CMR was very similar to that described above for whole-rock samples from the pyroxene-bearing assemblage, with the difference that only 3 milligrams of hand-picked biotite from this sample were prepared, with an irradiation time of 2 hours resulting in a calculated J factor of 0.000485.

Mass spectrometry was carried out on a modified MS-10 mass spectrometer and data corrections were applied as described in Roddick (1990). A shortened step-heating analysis was carried out on these samples, with three to four steps ranging between 500°C to 1550°C. Comparison of the ages derived from the last two or three steps helps in the assessment of the internal consistency of the age and provides a cross-check on the concordancy of the results. Errors in isotopic ratios were propagated and evaluated as outlined in Roddick (1988).

Samples HHB93-3203 and HHB93-3811, from rhyolite blocks in pyroclastic units of the biotite-bearing assemblage at localities east of Canyon Mountain, were prepared in a similar manner as a separate irradiation, with a resulting J factor of approximately 0.00185. Mass spectrometry of these samples was carried out on a VG3600 mass spectrometer, a magnetic sector mass spectrometer with 60° extended geometry equipped with a Faraday collector and electron multiplier. The signal on the latter is measured across a  $1 \times 10^9$  ohm resistor with a resulting gain, relative to Faraday, of approximately 50. Mass spectrometer sensitivity while using the electron multiplier is gain dependent, but is approximately at  $1.900 \times 10^{-9}$  cubic centimetres STP/V. Samples were loaded into foil packets and irradiated as described above, except that the corresponding monitor was Fish Canyon Tuff sanidine, with an age of  $28.03 \pm 0.1$  Ma (Renne *et al.*, 1995).

Upon return from the reactor, samples were split into two aliquots, loaded into separate 1.5 millimetre diameter x 4 millimetre deep holes in a copper planchet and placed under vacuum in a chamber topped with a Zn-Se window. This window is transparent to the beam of a Weck CO<sub>2</sub>, 45-watt surgical laser, which was stepped incrementally from 2 to 45 power watts before being optically attenuated by 1/20. Power density in the beam forms a Gaussian distribution, and thus the edges are clipped by a metal mask restricting the beam to approximately 150 millimetre diameter at the sample with roughly constant power distribution. The beam is manually "panned" for 1 minute around the hole to provide roughly even heating of the sample. Cross-checking of gas release spectra on standards step-heated in the MS-10/double vacuum furnace shows that the increasing CO<sub>2</sub> laser power mimics an increase in furnace temperature. Quantitative temperature calibration is not possible because sample geometry, size, opacity of sample to laser and other factors shift the heating spectrum to higher or lower absolute temperatures within any one hole.

**TABLE 1**  
**ARGON STEP HEATING DATA FOR SAMPLES RUN ON MS-10/FURNACE AT GEOLOGICAL SURVEY OF CANADA**

Temp (°C)	<sup>36</sup> Ar <sub>tr</sub>	<sup>37</sup> Ar <sub>Ca</sub>	<sup>38</sup> Ar <sub>Cl</sub>	<sup>39</sup> Ar <sub>K</sub>	<sup>40</sup> Ar	% Atmos <sup>40</sup> Ar	Apparent Age Ma±2 <sup>b</sup>	<sup>39</sup> Ar (%)
	x10 <sup>-9</sup> cm <sup>3</sup> STP <sup>a</sup>							
<b>HHB93-3710 (21.54 mg) J = .001874 ± 0.50 %, 1</b>								
500°	0.006	0.139	0.100	1.085	16.660	10.8%	45.7±0.4	11.2%
750°	0.024	1.175	0.452	5.383	80.190	9.0%	45.3±0.1	55.4%
1050°	0.005	0.923	0.140	1.811	25.690	6.1%	44.5±0.5	18.6%
1550°	0.016	0.906	0.125	1.433	23.980	19.9%	44.8±0.2	14.8%
Total <sup>c</sup>	0.050	3.140	0.820	9.710	146.500	10.5%	45.1±0.5	
Conc.(/g)	2.410	145.900	37.900	450.900	6803.0			
<b>HHB93-3306 (19.71 mg) J = .001868 ± 0.50 %, 1</b>								
500°	0.010	0.140	0.011	0.481	5.750	49.2%	20.4±0.6	5.7%
850°	0.021	1.561	0.047	5.146	83.710	7.5%	50.0±0.1	61.3%
1050°	0.004	0.594	0.088	1.922	29.330	4.4%	48.5±0.1	22.9%
1550°	0.010	0.429	0.049	0.843	14.960	19.4%	47.6±0.2	10.0%
Total <sup>c</sup>	0.040	2.720	0.200	8.390	133.700	9.9%	47.7±0.5	
Conc.(/g)	2.280	138.200	9.900	425.700	6786.0			
<b>HHB93-3501 (21.05 mg) J = .001861 ± 0.50 %, 1</b>								
500°	0.011	0.230	0.193	2.002	30.270	10.8%	44.7±0.2	21.4%
850°	0.018	2.246	0.522	5.975	84.890	6.2%	44.2±0.1	63.8%
1050°	0.003	0.881	0.056	0.660	8.980	8.7%	41.2±0.4	7.0%
1550°	0.009	1.287	0.075	0.724	12.050	21.3%	43.4±0.2	7.7%
Total <sup>c</sup>	0.040	4.640	0.850	9.360	136.200	8.7%	44.0±0.4	
Conc.(/g)	1.910	220.600	40.210	444.700	6470.0			
<b>HHB93-3005 (26.11 mg) J = .001851 ± 0.50 %, 1</b>								
500°	0.013	0.172	0.008	0.569	6.180	61.8%	13.8±0.5	6.3%
850°	0.016	2.407	0.024	6.966	113.060	4.3%	51.1±0.1	76.7%
1050°	0.003	0.728	0.048	1.151	17.680	5.3%	48.0±0.3	12.7%
1550°	0.008	1.434	0.042	0.401	8.270	30.0%	47.6±0.5	4.4%
Total <sup>c</sup>	0.040	4.740	0.120	9.090	145.200	8.3%	48.3±0.5	
Conc.(/g)	1.570	181.500	4.700	348.000	5561.0			
<b>95-CMR (3.1 mg) J = .000485 ± 0.50 %, 1</b>								
600°	0.005	0.023	0.000	0.005	1.660	85.2%	42.6±57.2	0.9%
970°	0.013	0.023	0.009	0.132	11.920	33.5%	52.0±0.7	23.7%
1550°	0.007	0.022	0.025	0.420	26.740	7.4%	50.9±0.6	75.4%
Total <sup>c</sup>	0.020	0.070	0.030	0.560	40.300	18.3%	51.1±0.9	
Conc.(/g)	8.060	21.780	11.010	179.400	13010.0			
<sup>a</sup> All gas quantities have been corrected for decay, isotopes derived from minor interfering neutron reactions and blanks. tr denotes trapped Ar. Ca, Cl, K denote Ar derived from these elements. <sup>40</sup> Ar denotes trapped plus radiogenic Ar. <sup>40</sup> Ar assumes a trapped argon component of atmospheric composition.								
<sup>b</sup> Errors from individual steps are analytical only and do not include the error in irradiation parameter J.								
<sup>c</sup> Includes the integrated age. The uncertainty in J is included in the error.								

**TABLE 2**  
**ARGON STEP HEATING DATA FOR SAMPLES RUN ON VG3600/LASER AT GEOLOGICAL SURVEY**

Power <sup>a</sup> (W)	<sup>36</sup> Ar <sub>tr</sub>	<sup>37</sup> Ar <sub>Ca</sub>	<sup>38</sup> Ar <sub>Cl</sub>	<sup>39</sup> Ar <sub>K</sub>	<sup>40</sup> Ar	% Atmos <sup>40</sup> Ar	Apparent Age Ma±2 <sup>c</sup>	<sup>39</sup> Ar (%)
	x10 <sup>-11</sup> cm <sup>3</sup> STP <sup>b</sup>							
HHB93-3203 Biotite, J = .0018188 ± 0.50 %, 1								
<i>Aliquot A</i>								
3W	0.436	0.055	0.051	0.682	130.420	98.7%	7.9±12.8	0.4%
5W	0.212	0.064	0.132	1.998	76.170	82.3%	22.0±1.9	1.2%
8W	0.165	0.055	0.116	1.682	65.830	74.2%	32.8±2.1	1.0%
10W	0.165	0.062	0.210	2.940	79.370	61.3%	34.0±1.1	1.8%
11W	0.376	0.136	0.695	9.513	235.310	47.2%	42.4±0.4	5.7%
15W	0.442	0.335	1.125	15.157	355.950	36.7%	48.1±0.4	9.1%
18W	0.491	0.676	2.247	30.317	618.570	23.5%	50.5±0.2	18.1%
20W	0.275	0.607	1.674	22.884	443.430	18.3%	51.2±0.2	13.7%
22W	0.113	0.330	0.677	8.897	172.850	19.3%	50.7±0.2	5.3%
25W	0.105	0.410	0.701	9.072	175.080	17.8%	51.3±0.3	5.4%
30W	0.136	0.962	0.915	11.277	218.130	18.4%	51.1±0.3	6.7%
35W	0.090	0.671	0.557	6.655	130.890	20.4%	50.7±0.5	4.0%
45W	0.103	0.970	0.919	10.966	202.440	15.0%	50.7±0.2	6.5%
Subtotal <sup>d</sup>	3.110	5.330	10.020	132.040	2904.400	31.6%	48.7±0.5	79.0%
<i>Aliquot B</i>								
3W	0.129	0.042	0.048	0.646	42.530	89.4%	22.7±8.0	0.4%
5W	0.108	0.069	0.205	2.899	67.160	47.4%	39.5±0.8	1.7%
8W	0.070	0.080	0.237	3.204	68.480	30.3%	48.2±0.7	1.9%
10W	0.043	0.079	0.180	2.370	49.640	25.6%	50.4±0.4	1.4%
11W	0.058	0.120	0.318	4.194	83.190	20.5%	51.0±0.3	2.5%
12W	0.028	0.101	0.162	2.070	40.630	20.4%	50.5±0.5	1.2%
15W	0.054	0.189	0.261	3.346	69.200	23.2%	51.3±0.4	2.0%
20W	0.063	0.396	0.524	6.887	127.810	14.7%	51.2±0.3	4.1%
25W	0.025	0.262	0.203	2.563	47.930	15.2%	51.3±1.1	1.5%
30W	0.039	0.331	0.392	5.235	94.810	12.2%	51.4±0.6	3.1%
45W	0.013	0.257	0.155	2.013	35.460	10.9%	50.8±0.6	1.2%
Subtotal <sup>d</sup>	0.630	1.930	2.680	35.430	726.800	25.6%	49.4±0.5	21.0%
<b>Total<sup>d</sup></b>	<b>3.740</b>	<b>7.100</b>	<b>12.700</b>	<b>167.470</b>	<b>3631.300</b>	<b>30.4%</b>	<b>48.8±0.5</b>	

<sup>a</sup>Laser power in watts, prior to 20x optical attenuation of beam

<sup>b</sup>All gas quantities have been corrected for decay, isotopes derived from minor interfering neutron reactions and blanks. tr denotes trapped Ar. Ca, Cl, K denote Ar derived from these elements. <sup>40</sup>Ar denotes trapped plus radiogenic Ar. <sup>40</sup>Ar assumes a trapped argon component of atmospheric composition. <sup>c</sup>All gas quantities have been corrected for decay, isotopes derived from minor interfering neutron reactions and blanks. tr denotes trapped Ar. Ca, Cl, K denote Ar derived from these elements. <sup>40</sup>Ar denotes trapped plus radiogenic Ar. <sup>40</sup>Ar assumes a trapped argon component of atmospheric composition.

<sup>c</sup>Errors from individual steps are analytical only and do not include the error in irradiation parameter J.

<sup>d</sup>Includes the integrated age. The uncertainty in J is included in the error

TABLE 2 Continued

Power <sup>a</sup> (W)	<sup>36</sup> Ar <sub>tr</sub>	<sup>37</sup> Ar <sub>Ca</sub>	<sup>38</sup> Ar <sub>Cl</sub>	<sup>39</sup> Ar <sub>K</sub>	<sup>40</sup> Ar	% Atmos <sup>40</sup> Ar	Apparent Age Ma±2 <sup>c</sup>	<sup>39</sup> Ar (%)
	x10 <sup>-11</sup> cm <sup>3</sup> STP <sup>b</sup>							
HHB93-3811 Biotite, J = .0018424 ± 0.50 %, 1 S.E.								
<i>Aliquot A</i>								
3W	0.746	0.079	0.097	1.676	231.010	95.5%	20.7±5.1	1.9%
5W	0.172	0.075	0.166	2.526	85.570	59.4%	45.1±1.5	2.9%
8W	0.130	0.093	0.280	4.165	105.210	36.6%	52.5±0.7	4.7%
10W	0.096	0.110	0.280	4.068	93.930	30.3%	52.7±0.8	4.6%
11W	0.140	0.273	0.512	7.144	157.290	26.3%	53.2±0.6	8.1%
12W	0.043	0.113	0.185	2.556	54.240	23.6%	53.1±0.6	2.9%
15W	0.045	0.167	0.202	2.777	58.460	22.8%	53.2±0.7	3.2%
20W	0.064	0.376	0.351	4.697	94.530	20.0%	52.8±0.4	5.3%
30W	0.018	0.157	0.030	1.102	22.850	23.4%	52.0±0.6	1.3%
45W	0.014	0.359	0.108	0.974	19.380	20.6%	51.8±1.2	1.1%
Subtotal <sup>d</sup>	1.470	1.800	2.210	31.690	922.500	47.0%	50.5±0.6	36.0%
<i>Aliquot B</i>								
3W	0.754	0.071	0.071	1.285	232.400	95.8%	25.0±8.8	1.5%
5W	0.141	0.096	0.245	3.577	97.080	42.8%	50.9±0.9	4.1%
8W	0.079	0.116	0.242	3.236	75.940	30.6%	53.4±0.8	3.7%
10W	0.061	0.131	0.192	2.473	58.160	31.0%	53.1±1.2	2.8%
11W	0.050	0.171	0.167	2.238	51.510	28.7%	53.8±1.1	2.5%
12W	0.020	0.119	0.071	0.892	20.630	29.0%	53.8±1.6	1.0%
15W	0.022	0.097	0.075	1.021	23.330	27.9%	53.9±1.0	1.2%
20W	0.027	0.079	0.057	0.860	21.880	36.2%	53.2±1.4	1.0%
45W	0.478	0.499	0.728	10.197	299.190	47.2%	50.8±0.5	11.6%
Subtotal <sup>d</sup>	1.630	1.460	1.850	25.780	880.100	54.8%	50.6±0.7	29.4%
<i>Aliquot C</i>								
3W	0.924	0.072	0.103	1.941	287.900	94.9%	25.0±7.0	2.2%
5W	0.242	0.109	0.291	4.516	138.630	51.6%	48.8±1.0	5.1%
8W	0.114	0.123	0.323	4.623	109.810	30.6%	54.0±0.5	5.3%
10W	0.073	0.130	0.264	3.644	81.590	26.4%	54.0±0.7	4.1%
11W	0.120	0.345	0.479	6.571	144.070	24.7%	54.1±0.5	7.5%
12W	0.029	0.112	0.130	1.805	38.650	22.5%	54.4±0.4	2.1%
15W	0.036	0.229	0.163	2.216	46.570	22.8%	53.2±0.5	2.5%
20W	0.050	0.231	0.227	3.162	66.470	22.3%	53.5±0.4	3.6%
30W	0.015	0.106	0.077	1.130	22.620	19.9%	52.5±1.1	1.3%
45W	0.013	0.106	0.060	0.829	16.870	22.3%	51.8±1.0	0.9%
Subtotal <sup>d</sup>	1.620	1.680	2.120	30.440	953.200	50.1%	51.2±0.7	34.6%
<b>Total<sup>d</sup></b>	<b>4.720</b>	<b>4.740</b>	<b>6.180</b>	<b>87.900</b>	<b>2755.800</b>	<b>50.5%</b>	<b>50.8±0.6</b>	

<sup>a</sup>Laser power in watts, prior to 20x optical attenuation of beam.

<sup>b</sup>All gas quantities have been corrected for decay, isotopes derived from minor interfering neutron reactions and blanks. tr denotes trapped Ar. Ca, Cl, K denote Ar derived from these elements. <sup>40</sup>Ar denotes trapped plus radiogenic Ar. <sup>40</sup>Ar assumes a trapped argon component of atmospheric composition.

<sup>c</sup>Errors from individual steps are analytical only and do not include the error in irradiation parameter J.

<sup>d</sup>Includes the integrated age. The uncertainty in J is included in the error

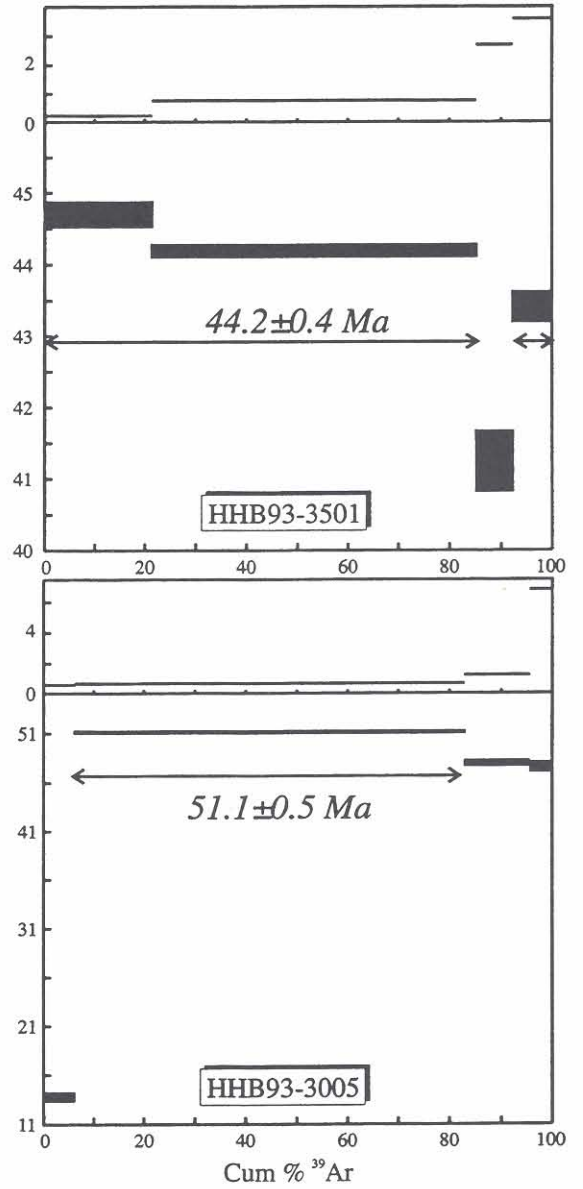
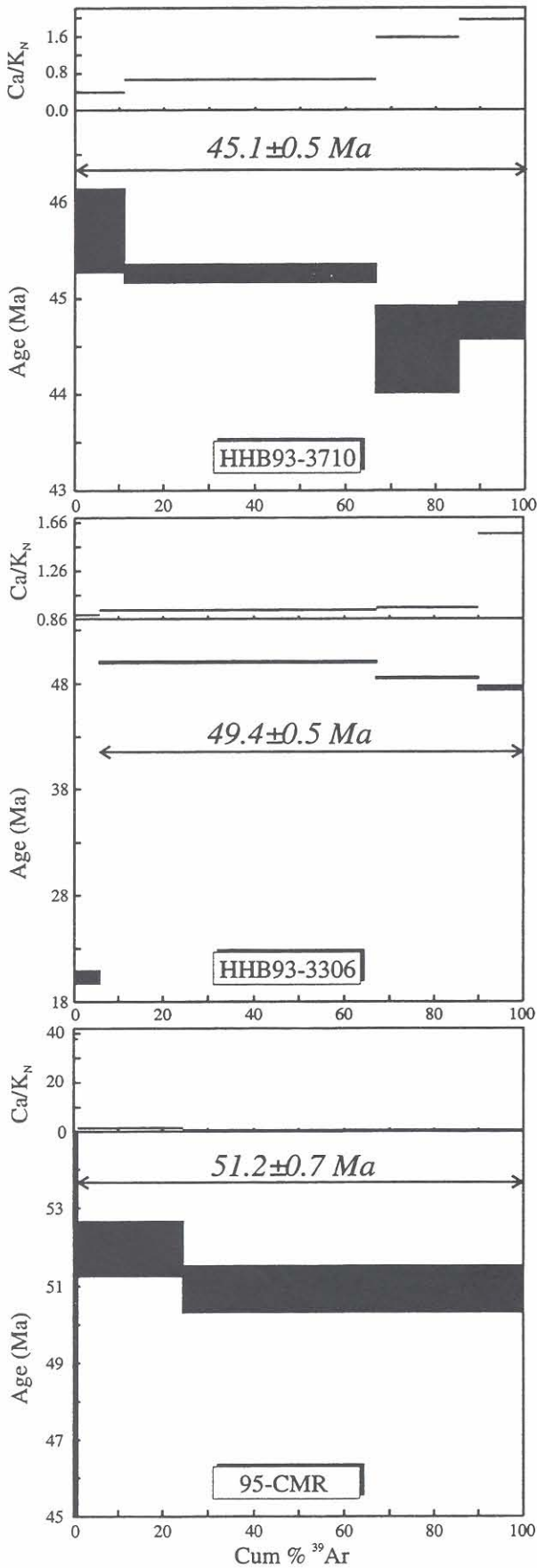


Figure 4. Gas release spectra for samples run with three to four steps of heating on MS-10/furnace at Geological Survey of Canada. All samples are whole-rock analyses except 95-CMR (lower left), which is a biotite separate. Data on individual gas fractions are not reproduced here, but are available from the laboratory upon request. All samples show a slight fall-off in age at the highest temperatures. This correlates with marked increases in Ca/K<sub>N</sub>, perhaps indicating the presence within the samples of an additional alteration phase that degasses at higher temperatures. Steps used for age picks are indicated on each plot.

The gas released is cleaned by passive equilibration of the gas with a getter filled with three SAEST<sup>TM</sup> NP-10 getters of ST707 alloy held at 400°C, as well as a cold getter of SAEST<sup>TM</sup> alloy 201 pellets for 2 to 5 minutes. Total extraction blank is approximately  $8 \times 10^{-12}$  cubic centimetres STP  $^{40}\text{Ar}$  for all steps. Argon peaks are sequentially scanned by computer-controlled switching of magnetic field, as monitored by a calibrated Hall probe (see Roddick, 1995 for details). Twelve scans of each mass were measured together with baselines taken 0.4 masses away from the  $^{36}\text{Ar}$  peak. Corrections to the measured peak intensities were carried out as described in Roddick (1990). Data reduction procedures for each aliquot follows Roddick (1988). Upon completion of each of the two aliquots of the sample, data were combined and treated as a single data set for analysis

by the inverse isochron method (Roddick *et al.*, 1980; error analysis follows Roddick, 1988) and integration of plateau portions of a gas release spectrum. Because data from the two samples presented in this paper are highly radiogenic and point towards an initial  $^{40}\text{Ar}/^{36}\text{Ar}$  value of 295.5, the data are presented as a single gas-release spectrum (consisting of two aliquots) for each sample. For reasons outlined in Roddick (1988), error in J factor measurement of  $\pm 0.5\%$  is only included in the final age determination.

Analytical data are presented in Tables 1 and 2. Analytical results are summarized in Figures 4 (MS-10 mass spectrometer/furnace) and 5 (VG3600 mass spectrometer/laser). The interpreted ages are similar to the age range of 47.6 Ma to 49.9 Ma obtained for the Wolf property (Andrew, 1988).

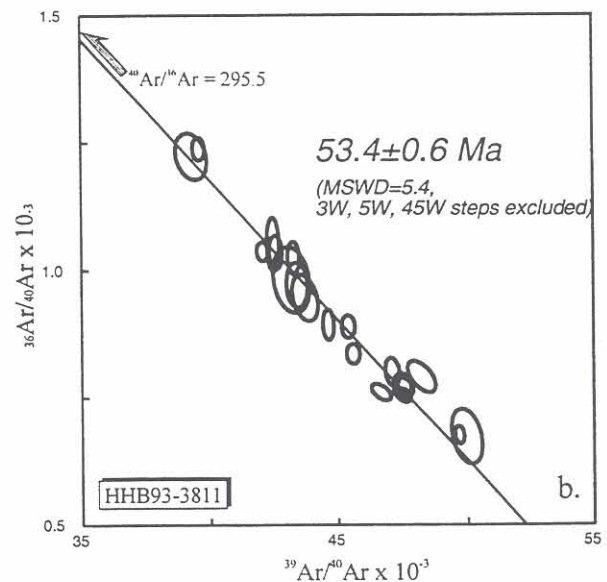
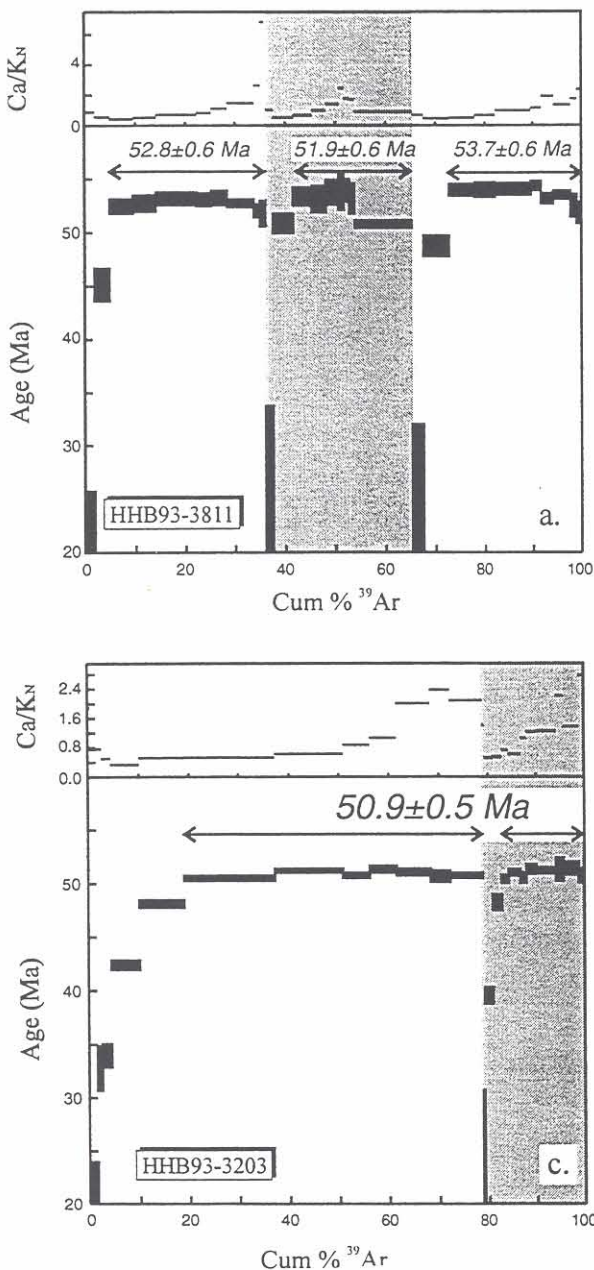


Figure 5. Results from samples run on VG3600/laser system at Geological Survey of Canada.

a. Gas release spectra for aliquots A, B and C from sample HHB93-3811 biotite. 300-500  $\mu\text{m}$ , strongly altered, mottled gold biotite was analysed, with each aliquot giving a different plateau age. Isotope systematics indicate argon loss in the first two low-temperature steps, while the highest temperature step of each aliquot appears to contain gas from an alteration phase (as indicated by increased  $\text{Ca}/\text{K}_N$ ).

b. An inverse isochron diagram of all aliquots with low and high-temperature steps removed results in an age of  $53.4 \pm 0.6$  Ma, the interpreted age of the sample.

c. Gas release spectra for aliquots A and B from sample HHB93-3203 biotite. Both aliquot plateau ages agree and the combined results give an age of  $50.9 \pm 0.5$  Ma.

The four samples taken from the pyroxene-bearing assemblage yielded ages ranging from  $51.1 \pm 0.5$  Ma to  $44.2 \pm 0.4$  Ma. Pyroxene-bearing volcanism in the Clisbako area was therefore active for at least 6 million years during Middle Eocene (Lutetian) time. The considerable range in ages for this assemblage, and their relatively silicic and viscous compositions, suggest that the lavas are reasonably close to a source vent. The presence of a circular highland which marks their outcrop area, and the associated magnetic high in the west-central part of the area (Teskey *et al.*, 1996; Shives and Carson, 1994), strongly suggest that the area was occupied by a large volcanic complex in Eocene time.

The number of samples analysed from this assemblage is insufficient to document the volcanic history of the area, but their individual ages and locations are of interest. Samples HHB93-3005 and HHB93-3306 are flow-laminated dacite taken from Toil Mountain and from an outcrop on the McFarland Creek road in the eastern-central part of the area. Both samples have suffered some surface alteration along flow laminae and their ages are less well constrained, but lie in the 48 to 52 Ma range. Sample HHB93-3710, from a colonnade at the extreme eastern edge of the Eocene outcrop area, returned a well constrained age of  $45.1 \pm 0.3$  Ma, consistent with the layered stratigraphy of a stratovolcano.

Sample HHB93-3501 was taken from Little Mountain, near the centre of the Eocene outcrop area and returned an age of  $44.2 \pm 0.4$  Ma, the youngest of the four ages and within error of the colonnade sample on the eastern margin (the age grouping may be due to the small number of samples analysed). The age and position of the Little Mountain sample suggest either that the volcano was not a true stratovolcano, or that there has been substantial subsidence of the central part of the edifice since formation.

The sample from Canyon Mountain (95-CMR) returned an age of  $51.2 \pm 0.7$  Ma and one sample of biotite rhyolite from a pyroclastic flow has an interpreted age of  $50.9 \pm 0.5$  Ma that lies within error of this date. This age distribution strongly suggests a single large pyroclastic phase of activity. However, the other pyroclastic sample, HHB93-3811, yielded mottled gold biotite which, despite a disparity in plateau ages (Figure 5), returned an age of  $53.4 \pm 0.6$  Ma. The sample does show some geological contamination by augite-bearing dacite, which significantly affects its chemical composition, but should have had little effect on the isotopic systematics of biotite. The age is interpreted as real; the phase of pyroclastic biotite-bearing volcanism was therefore at least 1.4 Ma in duration, or there was more than one period of such activity. It is also noteworthy that the intensely quartz-phyric units appear to postdate the other units of this assemblage (Richards and others, unpublished data).

Data obtained in this study are in agreement with data obtained for the eastern part of the study area by Rouse and

Mathews (1988) and with data obtained for the Quesnel area (Rouse and Mathews, 1979). Both areas returned ages of  $48.8 \pm 1.5$  Ma to  $49.8 \pm 1.7$  Ma for a biotite-bearing assemblage, which is within error of the two youngest rhyolite samples analysed in this study. Dacite samples from the Nazko area returned ages of  $48.7 \pm 1.7$  Ma and  $45.7 \pm 1.6$  Ma and dacites in the Quesnel area returned an age range of  $42.9 \pm 2.9$  Ma to  $41.6 \pm 2.9$  Ma. It should be noted that, in all three studies, the dacite ages while within error of those returned from biotite-bearing rocks, are younger. This is inconsistent with the great volume of dacitic accidental material in the rhyolitic pyroclastic rocks.

Metcalfe and Hickson (1995) interpreted the Clisbako area as the erosional remnant of a large volcanic edifice, on the basis of its subdued relief. However, this hypothesis of deep erosion is inconsistent with the presence of uneroded Eocene sedimentary rocks which formed after deposition of a large volume of volcanic material. A substantial thickness of Eocene volcanic rock probably underlies the central and western part of the area. The relatively subdued topography is either the result of considerable subsidence in the central part of the edifice or its inundation by an equivalent thickness of Chilcotin basalts.

Isotopic and field evidence indicate the occurrence of one, possibly two episodes of silicic pyroclastic volcanism with the associated extrusion of rhyolitic flow domes, preceded by a major phase of constructive dacitic volcanism and followed by 6 to 7 million years of intermittent dacitic eruptions. This history is consistent with the younger ages of two of the pyroxene-bearing assemblage, the roughly coeval ages (within error) of the two remaining pyroxene-bearing samples and the occurrence of large quantities of dacitic accidental fragments in the biotite-bearing pyroclastic rocks.

### PALYNOLOGICAL AGE OF MOAT FACIES

Seven samples from within the study area were submitted for palynological analysis to the Institute of Sedimentary and Petroleum Geology, Geological Survey of Canada, Calgary. Table 3 lists the pollen and spore flora found in each sample with their abundance (rare, few, common and abundant). Microscope slide co-ordinates for specimens are in an unpublished fossil report (White, 1993).

The flora assemblages are derived from epiclastic and related rocks from the moat facies of the Mount Clisbako volcano, all of which contain detrital biotite. The only local source of biotite is the Eocene biotite-bearing volcanic assemblage, therefore the floral assemblages are contemporaneous with or postdate the biotite-bearing volcanic rocks. The biotite-bearing assemblage has been constrained at  $51.4 \pm 0.7$  Ma by  $^{40}\text{Ar}/^{39}\text{Ar}$  analysis (*see above*).

TABLE 3  
PALYNOLOGY OF SELECTED MICROFLORA IN THE CLISBAKO MOAT FACIES

Sample number (Richards)	93/B/17-A	93/B/13-13	93/B/13-13	22/6/92/15a	22/6/92/15b	16/6/92RR	04/7/92 A	04/7/92 B
Sample number (White)	C-310131	C-310132	C-310132	C-310133	C-310134	C-310135	C-310137	C-310138
UTM N	5856400	5853600	5853600	5854100	5854100	5842400	5840200	5840200
UTM E	452000	452200	452200	449200	449200	461500	414500	414500
fraction	unscreened	unscreened	+20 µm	+20 µm	+20 µm	unscreened	+20 µm	+20 µm
<i>Acer</i>		(?) rare						
cf. <i>Aesculus</i>		few		few				
<i>Alnus</i> sp., 4 and 5 pore	few						common	
cf. <i>Betula</i>	rare							
cf. <i>Boisduvalia clavatites</i> Piel	rare, eroded							
Bombacaceae							rare	
<i>Carya juxtaporipites</i> (Wodehouse) Rouse		few		common	few	few		
<i>Carya</i> sp.					few			few
cf. <i>Cedrus</i> sp.						rare		
<i>Cercidiphyllum</i> sp.	rare				rare		cf; rare	rare
<i>Corylus</i> -type		rare						
<i>Cupuliferoideaepollenites liblarensis</i> (Thompson) Potonie		(?) few						
<i>Cupuliferoipollenites</i> sp. of Rouse and Mathews (1988, Plate 2, Fig. 6)	(?) rare			rare <sup>1</sup>				
Ericales								few
Hyphomycetes, hyphae		common <sup>2</sup>						
<i>Laevigatosporites</i> sp.		few		v. abundant				
Liliaceae	rare	few		rare				
<i>Liquidambar</i> sp.								rare
<i>Osmunda</i> sp.		few						rare
<i>Pachysandra/Sarcococca</i>	(?) rare	rare					(?) rare	
<i>Paraalnipollenites</i> cf. <i>P. alterniporus</i> (Simpson) Srivastava					rare			
<i>Picea</i> sp.				rare			few	common
Pinaceae (undifferentiated)		few		rare		common	common	

TABLE 3 Continued

Sample number (White)	C-310131	C-310132	C-310132	C-310133	C-310134	C-310135	C-310137	C-310138
<i>Pinus</i> sp.	few	abundant						common
<i>Pistillipollenites mcgregorii</i> Rouse					common	few	rare	
<i>Podocarpus</i> -type		cf. few					rare	rare
<i>Polyadosporites</i> sp.				few				
<i>Pterocarya</i> sp.				abundant			rare	
<i>Quercus</i> sp.		rare						
cf. <i>Rhoipites latus</i> of Mathews and Rouse (1984 Plate 1, Fig. 6)				rare				
<i>Sciadopitys</i> sp.		few					rare	cf. few
<i>Staphylosporonites</i> sp.		few						
<i>Syncolporites?</i> sp.			rare					
Taxodiaceae		common						
Taxodiaceae-Cupressaceae-Taxaceae (T-C-T)	common	abundant		common	common	common	common	abundant
<i>Tilia crassipites</i> Wodehouse		rare						
<i>Tilia</i> sp.					rare		few	
Tricolpate, new, of Rouse and Mathews (1988, Plate 2, Fig. 16)	rare							
Tricolporate A of Piel (1971)		fragment						
<i>Tricolporopollenites</i> sp.		few						
Triporate B of Piel (1971, Plate XVII, Fig. 150)		gemmate fragment <sup>3</sup>	rare					
<i>Tsuga canadensis</i> -type	few	few				rare		
<i>Tsuga</i> sp.				rare				rare
<i>Ulmus</i> -type				few				
fungal hyphae	common						few	

? denotes tentative identification

cf. denotes identification by close comparison

<sup>1</sup> Tricolporate, slight equatorial elongation 20/14 µm, psilate

<sup>2</sup> Many with microechinate or microverrucate ornamentation

<sup>3</sup> Fragment may be of *Boisduvalia clavatites* (Piel 1971)

Samples C-130134, -135, and -137 are inseparable in age based on the palynomorph assemblage. C-310138 has a non-diagnostic flora but is from the same locality as C-130137 and is of the same age. C-130134, -135 and -137 contain *Pistillipollenites mcgregorii*, a Late Paleocene to early Middle Eocene indicator (Mathews and Rouse, 1984). The value of *P. mcgregorii* as an indicator is emphasized by the fact that it was not observed in 200 palynological samples of Late Eocene to Oligocene age from the Amphitheatre Formation, Yukon Territory (Ridgeway *et al.*, 1995). The presence of *Tilia* pollen in C-130134 and -137 limits the maximum age of those samples to Eocene (Mathews and Rouse, 1984). The presence of *Paraalnipollenites alterniporus* in C-130134 is consistent with an Early to early Middle Eocene age range. The age of these four samples is in agreement with the  $^{40}\text{Ar}/^{39}\text{Ar}$  age of 51 Ma on the biotite-bearing lithological assemblage.

C-130132 lacks *P. mcgregorii*. It contains cf. *Aesculus* pollen, found in late Eocene beds at Cheslatta Falls (Rouse and Mathews, 1988). Tricolporate A and Triporate B of Piel (1971) were described in a palynomorph assemblage from the Australian Creek Fm. (Piel, 1971; Rouse and Mathews, 1979). The Australian Creek Formation assemblage, formerly considered to be of early Oligocene age (Piel, 1971; Rouse and Mathews, 1979), is now correlated to the Late Eocene (Ridgeway *et al.*, 1995), with the possibility that the assemblage extends into the Oligocene. Thus, C-130132 is younger than the samples described above, and is of Late Eocene or possibly Early Oligocene age. C-130131 has a very sparse assemblage, but contains *Boisdu-*

*valia clavatites*, an element of the Australian Creek Formation assemblage from central British Columbia described by Piel (1971). It is probably contemporaneous with C-130132. The significantly younger age of these samples may indicate a late phase of volcanism, but there is no isotopic or field evidence for such an event taking place. More probably, the provenance of biotite in these later rocks is the result of its recycling in an epiclastic environment, close to the source.

### CHILCOTIN GROUP BASALTIC ROCKS

Relatively well exposed basaltic lava flows occur in most of the valleys in the study area. These lavas are distinctively fresh in appearance and commonly show well developed colonnades and flow tops. Phenocrysts are most commonly olivine; less commonly plagioclase and rarely augite. They were assigned by Tipper (1959, 1969) to the Chilcotin Group and were also described by Mathews (1989). The ages of all the basaltic flows have not been documented, but Hunt (1992) described plant fossils in terrestrial sedimentary layers within the basaltic pile which are consistent with an Early Miocene age. No isotopic ages are available for flows within the area and some may be considerably younger. The basalts do not mask paleotopography, as they do in the plateau area to the west and south of the Clisbako highland; rather they fill paleovalleys, in places to depths of 200 metres or more (Hunt 1992), frequently covering eroded areas of less resistant Eocene rock and forming a protective cap. It should be noted that these

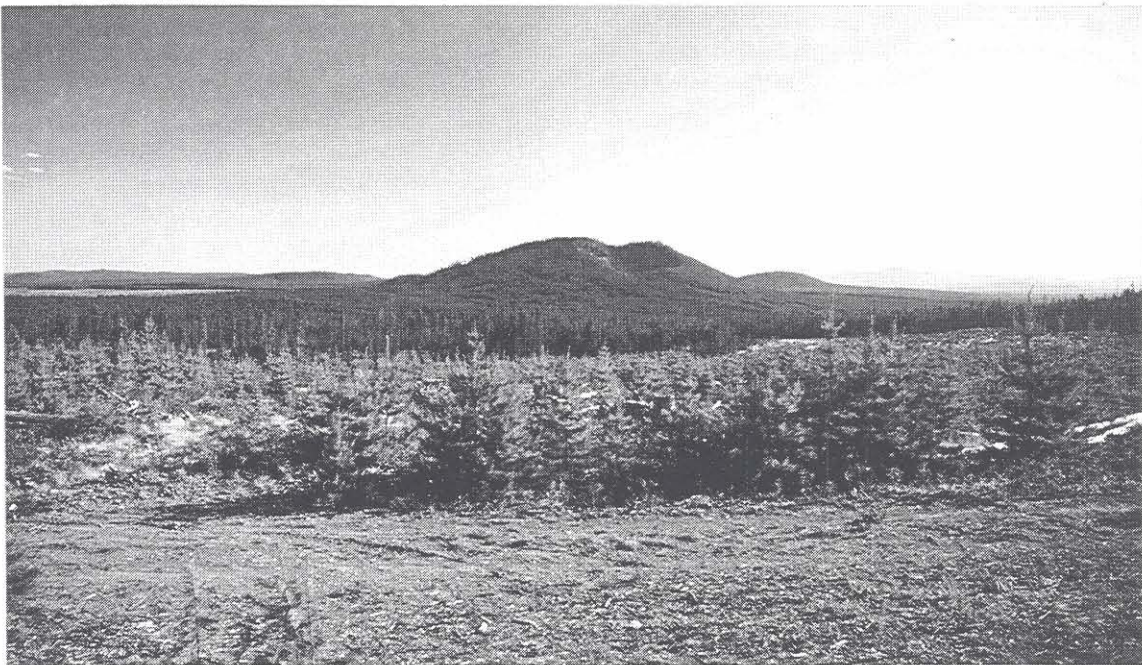


Photo 9. Relict cinder cones break the flat topography of the Chilcotin plateau lavas. In the foreground is Cleft Hill, one of the cones interpreted as a source for the lavas. The Chilcotin basalts overlie the two Eocene assemblages, filling ancient valleys and swamping the Eocene volcanic edifice.

lavas may mask significant epithermal exploration targets in the area.

Tipper (1959, 1969) noted the presence of a number of small cinder cones, which are probable source vents for the lavas. Several such structures were discovered during the course of fieldwork and may be more abundant than suggested by Tipper's mapping. Sharp, discrete magnetic anomalies over the Chilcotin Plateau to the southwest are coincident with small hills and may mark the locations of numerous Chilcotin vents. Tipper (personal communication to T.A. Richards) noted that some of the cinder cones present in the area and elsewhere on the Chilcotin Plateau may be considerably younger than their assumed age and represent part of the volcanism associated with the Anahim Belt.

One such cone (Cleft Hill) lies southwest of the Eocene outcrop area (Figure 2; Photo 9) and was examined in 1994. It has a central crater which is open to the north. Rocks exposed on the crater wall comprise interlayered agglutinate and vesicular basalt blocks. The cone appears to have a very low proportion of scoriaceous material, compared to the 7200-year-old Nazko cone, in the northeast of the area. The latter was described by Souther *et al.* (1987) and is outside the scope of the present study.

### INFERRED STRUCTURES

The Clisbako area is a glaciated area of low relief and poor outcrop; recessively weathering units and structures are very rarely exposed. The structural trends are therefore inferred from magnetic anomalies (Geological Survey of Canada, 1994; Shives and Carson, 1994) and by subtle variations in topography. Two predominant structural trends occur in the area. The most continuous magnetic lineaments have a northwest trend and are associated with a topographic "grain" which can be traced through the area and for a significant distance along strike.

A second set of strong magnetic anomalies trend north-northeasterly to northerly across the study area and also occur on the Chilcotin Plateau to the west and south. This set of anomalies is less continuous, but many of them cross the northwest-trending set without apparent displacement. Neither of the sets were observed in outcrop and neither their absolute and relative ages nor their senses of movement are known. The north-northeast structures are interpreted as extensional faults, analogous to basins and range and possibly hosting feeders either to the Eocene volcanic rocks or to the Chilcotin Group basalts. Extensional movement on these inferred structures could have taken place with associated strike slip reactivation of a northwest-trending fault set.

A third inferred structural trend is represented by two west-northwest-trending magnetic discontinuities north and south of the Toil Mountain anomaly. The more northerly is an extension of a persistent magnetic discontinuity along the trend of the Anahim volcanic belt, the other is

poorly defined and discontinuous. Both anomalies may represent westerly trending splays from the northwest-trending structures; their age is also unknown. The lack of age data for all potential structures in the area, precludes assessment of their relative potential as exploration targets, but if epithermal mineralization in the area is structurally controlled, the intersections of structures, particularly northwest trending and west trending, would be high-potential exploration targets.

Some non-linear anomalies in the study area are interpreted as edge effects of the more strongly magnetized Chilcotin Group flows. Spot anomalies coincident with small hills on the Chilcotin Plateau to the southwest are interpreted as eruptive centres for the Chilcotin Group basalts. These anomalies will mask geophysical exploration targets in the underlying Eocene rocks.

## CHEMICAL AND PETROGRAPHIC ANALYSIS OF THE CLISBAKO VOLCANIC COMPLEX

### PETROGRAPHY

Sixty-six samples from the area were examined in thin section. Of these samples, eleven were of Chilcotin Group basalts, the remainder from Eocene intermediate flows, flow breccias and related tuffaceous sedimentary rocks.

The Chilcotin basalts, although not the focus of the study, are described briefly here. The lavas are weakly to moderately porphyritic. Phenocryst assemblages comprise olivine, titaniferous augite and plagioclase. Where proximal to a vent, the basalts are often strongly porphyritic and/or xenophytic. On the western slopes of Canyon Mountain, they contain many xenoliths of chromian ilmenite, probably with trace chrome spinel; associated olivine and pyroxene xenocrysts are also abundant.

Distal Chilcotin lavas are less easy to distinguish in outcrop from the underlying Eocene dacitic volcanic rocks; lavas of both assemblages show well developed colonnades, are glaciated and as a result do not have flow surface features. Olivine, which occurs in the basaltic lavas, is often not visible in hand specimen and epidote alteration after plagioclase can be mistaken for olivine in a cursory examination of a dacite outcrop. The only consistent difference in appearance between the two lithologies is the ubiquitous dictytaxitic groundmass of the Chilcotin basalts, in contrast with the microcrystalline to glassy groundmass of Eocene dacites. Even where the basalt groundmass is finer grained, or microcrystalline, it is usually felted, while the dacites exhibit a moderate to strong trachytic crystal alignment, flow banding or flow folding.

### PYROXENE-BEARING ASSEMBLAGE

Samples of the pyroxene-bearing assemblage are weakly porphyritic to aphyric and monotonous in their phenocryst mineralogy. Phenocrysts rarely exceed 1 milli-

metre. The most abundant phenocryst phase is subhedral to euhedral plagioclase, commonly with strong oscillatory zoning, forming as much as 10% of any sample. Epidote alteration is common, but rarely pervasive. Larger plagioclase crystals contain intensely corroded cores (Photo 10). Core compositions, determined optically by the albite-Carlsbad method, range from An<sub>50</sub> to An<sub>55</sub>, with rare occurrences of cores as sodic as An<sub>30</sub>. Non-corroded rims exhibit pronounced oscillatory zoning and range in composition from An<sub>67</sub> to An<sub>62</sub>, the latter value at the rims. Microphenocrysts and groundmass plagioclase are in apparent equilibrium with these rims.

Pyroxene phenocrysts rarely comprise more than 5% of the whole rock and never more than 10%. Augite phenocrysts are usually more common, often with exsolution lamellae of orthopyroxene, but the latter phase also occurs as discrete phenocrysts. Phenocrysts of both pyroxene phases are euhedral to subhedral, with unaltered cores; both exhibit oscillatory zoning, faint in the orthopyroxene, often strong in the clinopyroxene and indicative of a significant titanium content (Photo 11). Pyroxene phenocrysts are rarely in contact with plagioclase, but the two phases are mutually interpenetrant, indicating cotectic crystallization.

Hornblende phenocrysts occur rarely in the pyroxene-bearing rocks, in some cases as equant, possibly uraltitic

phenocrysts after clinopyroxene or orthopyroxene and rimmed with iron-titanium oxide. A few samples from the eastern edge of the Eocene outcrop contain prismatic phenocrysts of euhedral to subhedral oxyhornblende, with

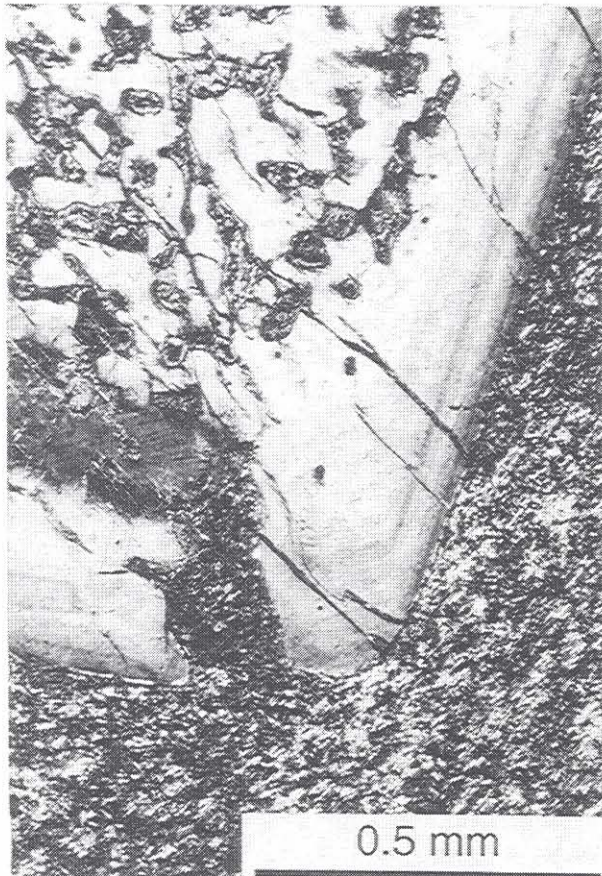


Photo 10. Corroded core of plagioclase phenocryst, with a fresh rim showing strong oscillatory zoning. Crossed polars.

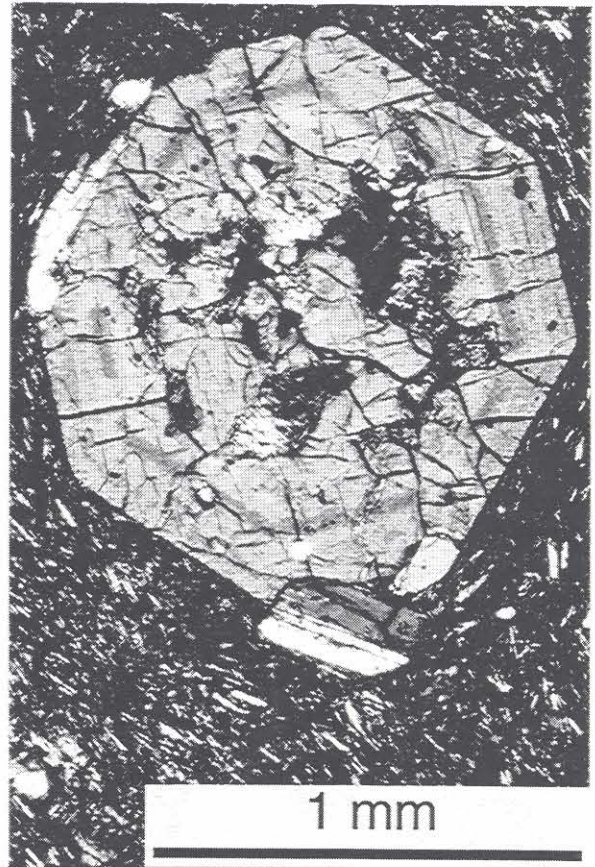


Photo 11. Euhedral titaniferous clinopyroxene with oscillatory zoning. Crossed polars.

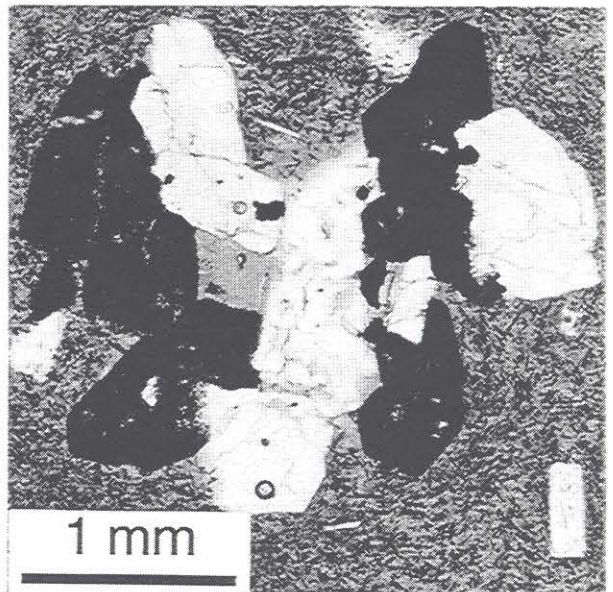


Photo 12. Glomerocryst in pyroxene-bearing lava, comprising corroded plagioclase phenocrysts and pseudomorphs after hornblende. Plane polarised light.

strongly oxidized rims. Most commonly, discrete crystals of hornblende are peripherally or pervasively replaced by a fine-grained intergrowth of alteration products or, rarely, by pyroxene.

Glomerocrysts, cored by anhedral clinopyroxene and orthopyroxene and rimmed with corroded plagioclase, are common in samples of the pyroxene-bearing assemblage. Relict outlines of pervasively altered euhedral to subhedral hornblende crystals were seen in a few sections (Photo 12). Relict phenocrysts of olivine, usually partially or completely replaced by pyroxene, are present in more mafic samples.

Apatite and zircon are rarely present in the phenocryst assemblage, although microphenocrysts of both phases are included in clinopyroxene. Apatite phenocrysts are as much as 0.1 millimetre in length, while microphenocrysts of zircon are volumetrically insignificant.

### BIOTITE-BEARING ASSEMBLAGE

Eight of the Eocene samples examined in thin section were taken from outcrops of the biotite-bearing assemblage. The assemblage is defined by the presence of magmatic biotite, either fresh or exhibiting replacement due to hydrothermal alteration. In all but one sample, the biotite occurs as phenocrysts, euhedral to subhedral and as large as 2 millimetres across (Photo 13). In rare cases, biotite and plagioclase coexist as microphenocrysts.

Hornblende phenocrysts are common in the biotite-bearing rocks and are often peripherally replaced by magmatic biotite (Photo 14). Hornblende is infrequently intergrown with plagioclase of intermediate composition; the two phases are probably coeval and are certainly older than the biotite. The latest phenocryst phases are rare, subhedral potassium feldspar (orthoclase, possibly after sanidine; Photo 15) and rare rounded quartz with well developed magmatic embayments (Photo 16). Both phases

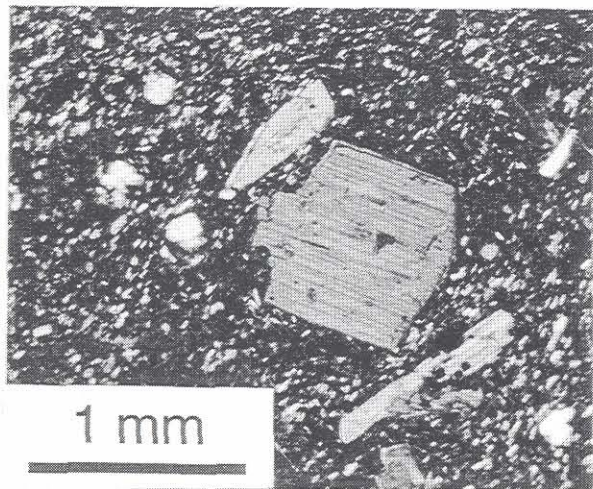


Photo 13. Euhedral biotite phenocryst, with two elongate hornblende phenocrysts, in lava of biotite-bearing assemblage. Crossed polars.

enclose one or more of the earlier phenocrysts. Apatite and zircon occur as rare microphenocrysts, with an undetermined position in the crystallization sequence.

Larger plagioclase crystals in rocks of the biotite-bearing assemblage contain intensely corroded cores (Photo 17), as do those in the pyroxene-bearing assemblage. Core



Photo 14. Euhedral hornblende phenocryst in rhyolite, peripherally replaced by biotite (bi). Biotite also occurs as discrete phenocrysts. At lower left is a large plagioclase crystal with corroded core and strongly zoned rim. Crossed polars.

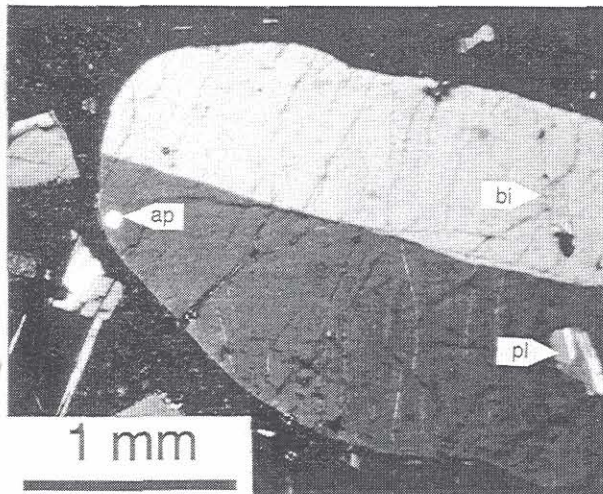


Photo 15. Potassium feldspar phenocryst, enclosing phenocrysts of plagioclase (pl), biotite (bi) and apatite (ap). Plagioclase also includes biotite. Crossed polars.

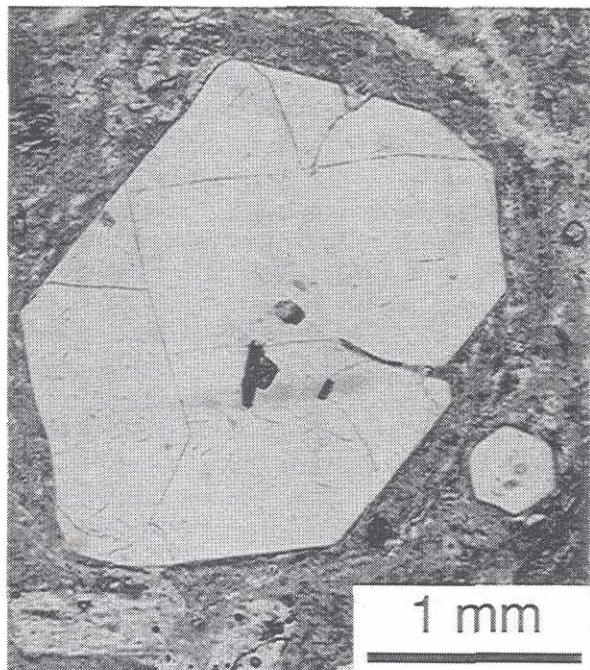


Photo 16. Quartz phenocryst with magmatic embayment and including a biotite phenocryst. Plane polarised light.

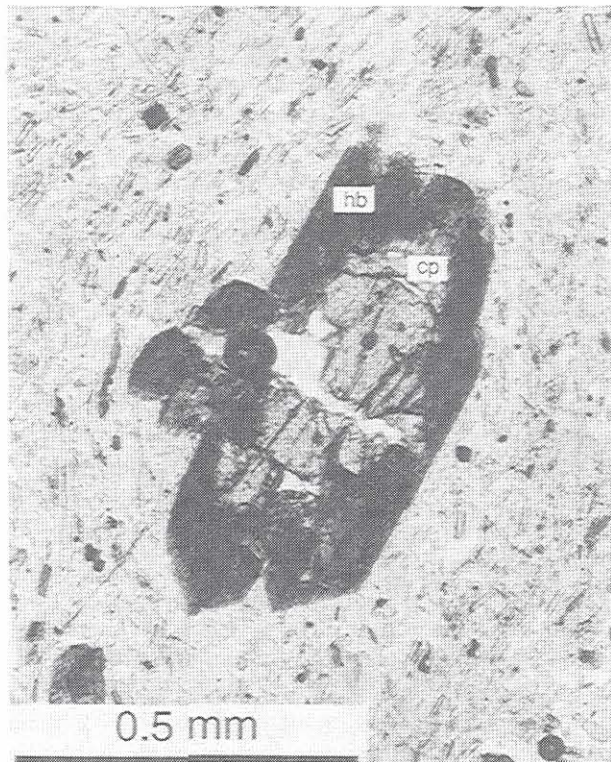


Photo 18. Clinopyroxene xenocryst with overgrowth of hornblende, possible evidence of magma mixing or, more probably, contamination. Plane polarised light.

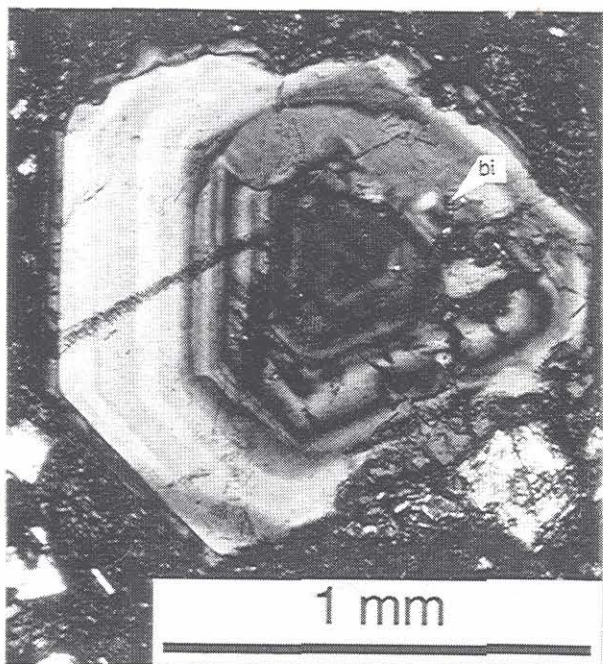


Photo 17. Corrodged core of plagioclase phenocryst in biotite-bearing assemblage, with a fresh rim showing strong oscillatory zoning. A small crystal of biotite (bi) is included in the core. Crossed polars.

and rim compositions, determined optically, are more variable than in the pyroxene-bearing assemblage; cores range from An<sub>65</sub> to An<sub>35</sub> and non-corrodged rims (with strong, oscillatory zoning) range from An<sub>55</sub> to An<sub>48</sub> at the rims. Microphenocrysts and groundmass plagioclase are in apparent equilibrium with these rims.

One sample (HHB94-5117) contains subhedral clinopyroxene crystals, with overgrowths of hornblende (Photo 18). This sample is somewhat more mafic than others of this assemblage and of atypical chemical composition. Nearly all the other samples examined contain small (2-5 mm) aggregates of corroded plagioclase and anhedral amphibole, identical in texture and size to those found in samples of the pyroxene-bearing assemblage. The sample may be the product of magma mixing, but the viscosities of potential parent magmas are probably too high to allow for efficient mixing (J.A. Roddick, personal communication, 1996). More probably, the sample is a product of contamination or assimilation of solid material (including previous intrusions) during ascent.

## CHEMISTRY

Sixty-seven samples were selected for chemical analysis, eleven from the Chilcotin Group basalts and the remainder from the Eocene Clisbako volcanic rocks. Chemical variations in the Chilcotin Group lavas are outside the scope of this study. Seven of the Eocene samples were biotite-bearing; the remaining 49 were from the pyroxene-bearing assemblage. The presence of alteration and occurrence of incognate xenocrysts were also used to group samples. Analyses were carried out by Chemex Labs, using x-ray fluorescence spectrometry. Analytical results for the

Clisbako volcanic rocks analysed in this study are not presented here but are available upon request from the Geological Survey of Canada. Data for 31 additional samples from the Clisbako area, made available by courtesy of Inmet Mining Corporation, are included in the chemical variation diagrams for comparison, but are not included in the petrologic discussion.

The Clisbako volcanic rocks are fairly typical of the Eocene Ootsa Lake Group in major element composition. They are subalkaline on a standard alkali-silica plot (Figure 6). The majority of samples in the pyroxene-bearing assemblage are dacites and nearly all of the biotite-bearing assemblage are rhyolites. On an AFM diagram (Figure 7) the samples lie in the calcalkaline field and with one exception, in the high-potassium field a  $\text{SiO}_2$ - $\text{K}_2\text{O}$  diagram (Figure 8). In these respects, the samples are typical of all Eocene volcanic rocks in the Interior Plateau (*cf.* Andrew, 1988; Drobe, 1991; Green, 1990; Smith, 1986).

Studies in the Interior Plateau to date have identified stratigraphic units such as the Ootsa Lake Group, Kamloops Group and Endako Group. These are valid stratigraphic definitions within their type areas, but these roughly coeval volcanic rocks overlie an area equivalent to that covered by the Cascades volcanoes. It is extremely unlikely that intermediate or silicic volcanic rocks from a single source would cover such a large area and far more probable that volcanic activity took place at a number of

discrete centres (volcanoes). In the latter case, volcanic stratigraphy would vary greatly between type sections (Alldrick, 1989). The location of volcanic paleocentres *within* a stratigraphic division must therefore be a priority in any study of the Eocene volcanic rocks of the Interior Plateau. The presence or absence of paleocentres also affects the economic potential of an area; epithermal mineral deposits such as that at Blackdome require a heat source.

Circumstantial evidence for the presence of a volcanic centre in the Clisbako area comprises the topographic expression of the Eocene units, the pronounced magnetic signature over Toil Mountain (Geological Survey of Canada, 1994; Teskey *et al.*, 1996; Shives and Carson, 1994) and the proximal nature of the volcanic deposits of both biotite-bearing and pyroxene-bearing assemblages. Evidence of a discrete chemical evolution for the Clisbako volcanic rocks would be conclusive evidence for their production from a discrete volcanic centre. A further test of the hypothesis of an Eocene volcanic centre would be the observed variations in trace element chemistry consistent with fractionation of phases with distinctive chemical compositions. If the chemical variation in unaltered rocks were predictable, lithochemical studies for areas of high exploration potential would be feasible.

Chemical evidence for a common origin for a discrete suite of volcanic rocks is provided by constant ratios of

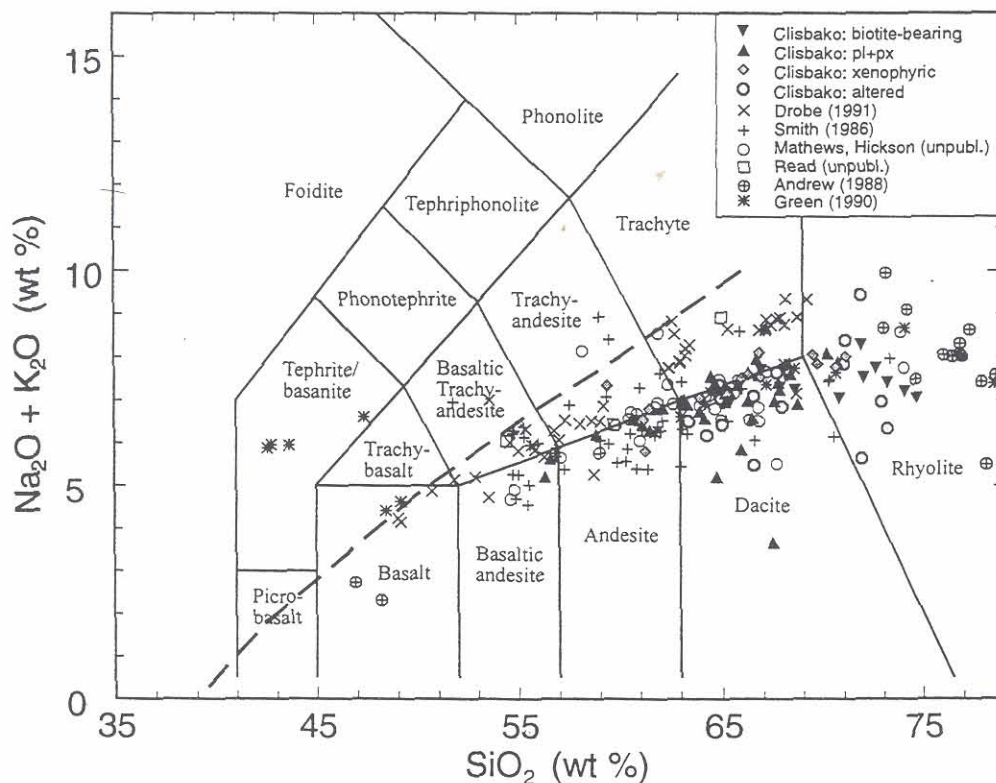


Figure 6. Weight percent silica against weight percent total alkalis after Irvine and Baragar (1971) and LeMaitre (1989). The Eocene rocks from the Interior Plateau lie in the oversaturated and saturated parts of the subalkaline field; those from Clisbako all lie reasonably close to the boundary, except for altered samples.

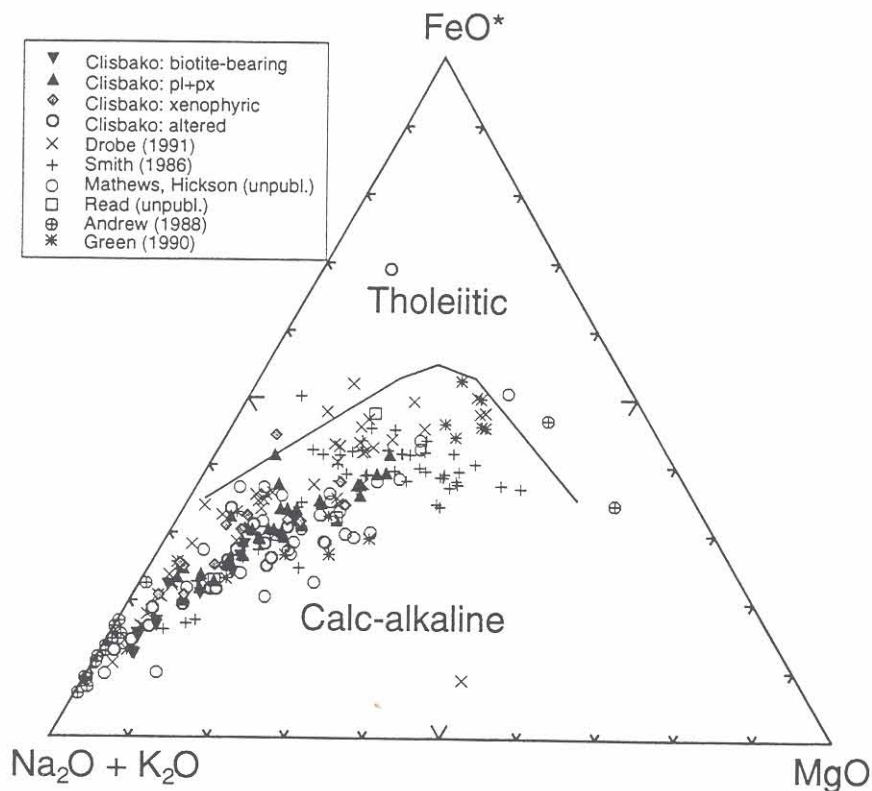


Figure 7. AFM diagram after Irvine and Baragar (1971). Nearly all samples from the Interior Plateau lie in the calcalkaline field.

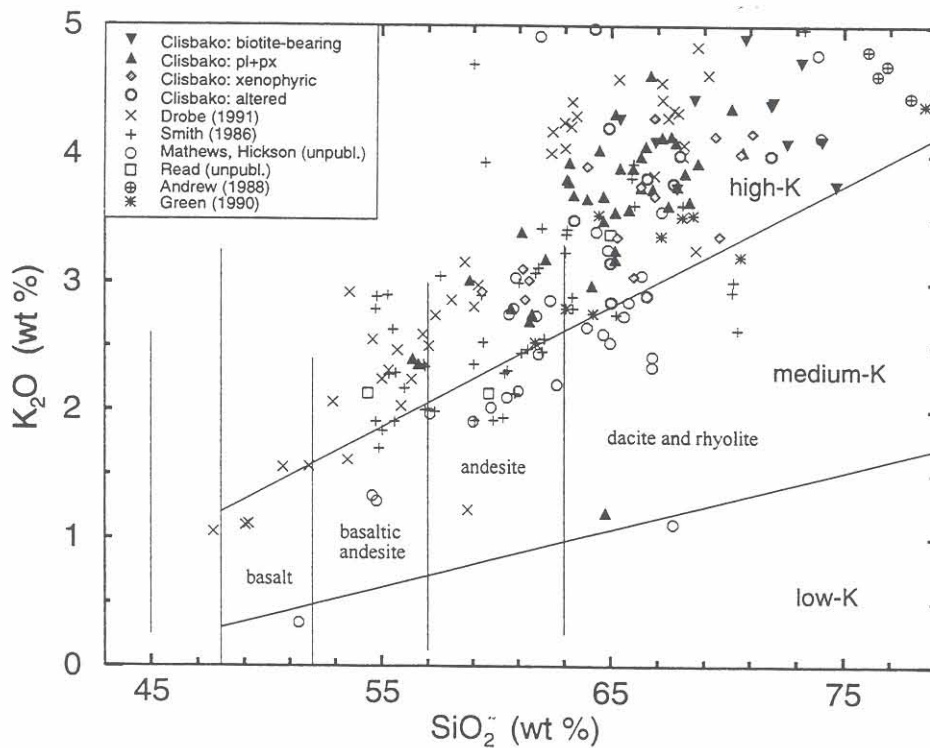


Figure 8. Weight percent SiO<sub>2</sub> against K<sub>2</sub>O after leMaitre (1989). With few exceptions, the Eocene lavas of the Interior Plateau lie in the high-potassium field

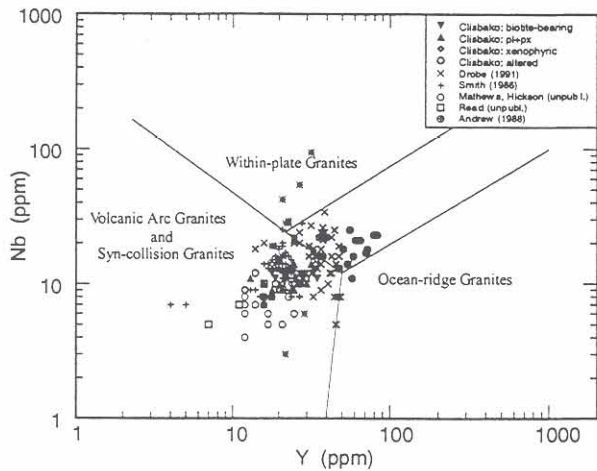


Figure 9. Yttrium vs. niobium after Pearce *et al.* (1984), for granitoid rocks. The majority of the intermediate and felsic volcanic rocks in the Interior Plateau lie in the same field as volcanic arc or syn-collision granites.

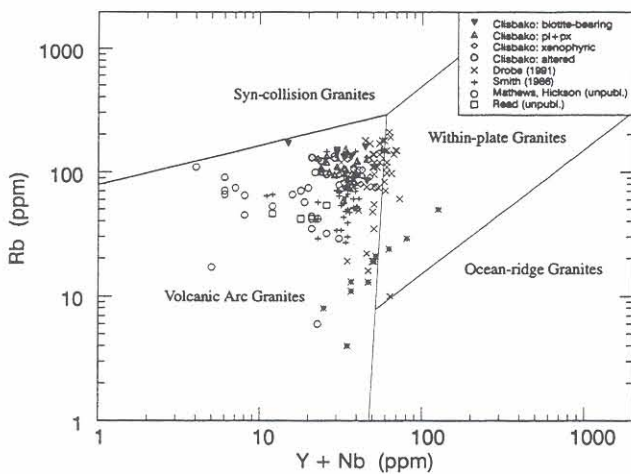


Figure 10. Yttrium+niobium against rubidium after Pearce *et al.* (1984), for granitoid rocks. The majority of the intermediate and felsic volcanic rocks in the Interior Plateau lie in the same field as volcanic arc granites.

conserved elements, that is, elements which are not involved in the formation of phenocryst or xenocryst phases (Russell and Nicholls, 1988). In the Interior Plateau, the available major element data (Figures 6-8) indicate that the volcanic assemblages are of similar composition. Moreover, the occurrence of potassium feldspar, apatite and titaniferous mafic phases in the Clisbako volcanic rocks suggests that no suitable candidates for a conserved constituent exist among the major elements.

Trace element abundances in Eocene rocks have only been determined in a few cases (Andrew, 1988; Drobe, 1991; Smith, 1986; Hickson and Mathews, unpublished data; Read, unpublished data) and for different groups of trace elements. Two slightly differing data sets (no Rb data

exist for Andrew's samples), plotted after Pearce *et al.* (1984) on granitoid discrimination diagrams (Figures 9 and 10), indicate that trace element compositions of the Interior Plateau lavas lie within the field of volcanic arc granites. Exceptions are the majority of Andrew's (1988) samples from close to the Wolf deposit. Only three of these samples lie within the field covered by the majority of the Eocene volcanic rocks. Most of the unaltered samples from the Clisbako area are similar in trace element composition to other samples from the Interior Plateau.

Ratios of incompatible large-ion lithophile and high field strength elements in the two Clisbako volcanic assemblages are relatively constant (Figures 11 and 12). By contrast, samples taken from a wide area of the Interior Plateau show a correspondingly wide distribution of incompatible element concentrations. Both assemblages of the Clisbako Volcanic rocks lie in fields discrete from other Eocene samples and reasonably closely constrained, interpreted as evidence for a discrete origin for both these assemblages and therefore the existence of a volcanic centre in the Clisbako area. The ratios of the high field strength elements yttrium, niobium and zirconium are most closely constrained and suggest that these elements are conserved in the Clisbako magmas.

A conserved constituent in any system is a constituent that is not removed or augmented by any of the processes affecting that system. The effect of closure (the summing of chemical compositions in that system to 100%) results in non-linear chemical variation diagrams (Russell and Nicholls, 1988). Normalization of the chemical components of any system to a conserved component allows for treatment of chemical or isotopic variation in the system using a linear model. The method is identical to that used for any isotopic system which generates an isochron, such as Rb-Sr,  $^{87}\text{Rb}$  and  $^{87}\text{Sr}$  being the variable constituents and  $^{86}\text{Sr}$  being the conserved constituent, for any given suite of samples.

Phenocryst phases present in the Clisbako volcanic rocks have distinct ranges of chemical variation. In the case of the pyroxene-bearing assemblage, chemical variation in the rocks may be expressed by the removal of plagioclase ( $\text{CaAl}_2\text{Si}_2\text{O}_8\text{-NaAlSi}_3\text{O}_8$ ), orthopyroxene ( $\text{Mg}_2\text{Si}_2\text{O}_6\text{-Fe}_2\text{Si}_2\text{O}_6$ ) and clinopyroxene ( $\text{CaMgSi}_2\text{O}_6\text{-CaFeSi}_2\text{O}_6$ ).

Using phase composition matrices (Russell and Stanley, 1990), axis coefficients were determined for an x-y graph of cation proportions upon which all chemical variations due to addition or subtraction of any or all of these phases will produce a chemical trend with a slope of 1. The axis coefficients to test for all species of feldspar are, for the x-axis,  $(\text{Al})/\text{Zr}$  and for the y-axis,  $(2\text{Ca}+\text{Na}+\text{K})/\text{Zr}$ . Similarly, the axis coefficients to test for plagioclase and pyroxene are, for the x-axis,  $(\text{Si})/\text{Zr}$  and, for the y-axis,  $(\text{Ca}+\text{Fe}+\text{Mg}+\text{Mn}+2.5\text{Na}+0.5\text{Al})/\text{Zr}$ .

On the plagioclase-pyroxene graph, for example, the slope  $dy/dx$  produced by separation of albite ( $\text{NaAlSi}_3\text{O}_8$ )

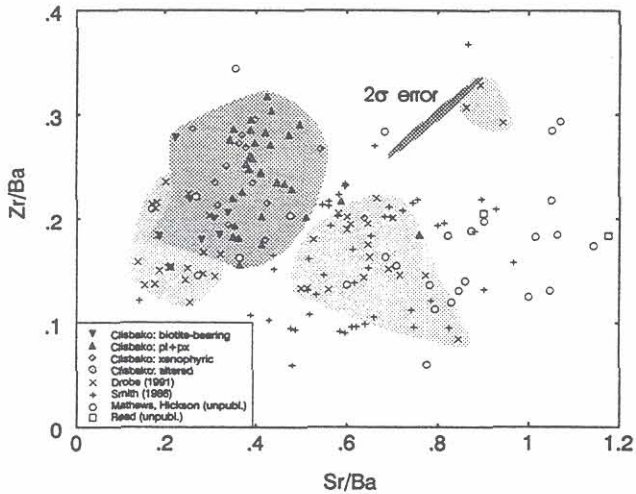


Figure 11. Sr/Ba vs. Zr/Ba plot (molecular proportions) for Eocene volcanic rocks of the Interior Plateau. Both assemblages of the Clisbako volcanics lie in fields distinct from the wide range of ratios in other suites.

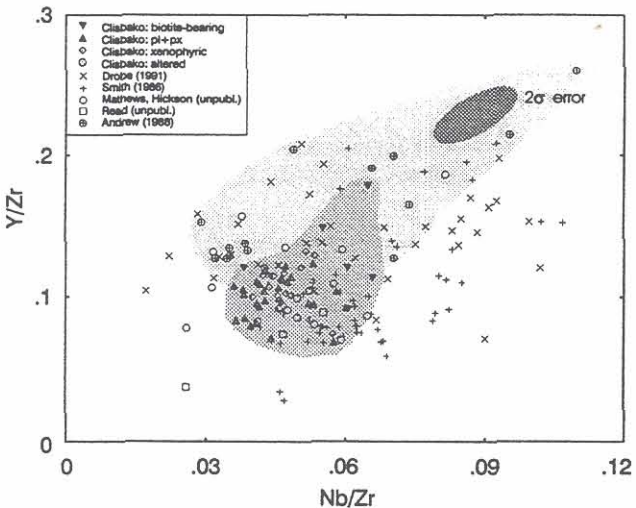


Figure 12. Ratios of high field strength incompatible elements for Eocene volcanic rocks of the Interior Plateau.

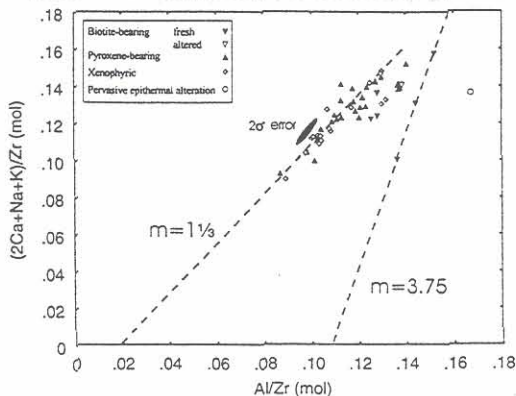


Figure 13. Pearce element ratio test diagram for feldspar for the Clisbako volcanics. Both assemblages fail this test, indicating that fractionation of plagioclase cannot account for the chemical variation in either assemblage.

would be  $(2.5 \times 1 \times \text{Na} + 0.5 \times 1 \times \text{Al}) / (3 \times \text{Si}) = 1$ . The hypothesis that the compositional range of the pyroxene-bearing assemblage is derived from fractionation (or assimilation) of feldspar, or of plagioclase and pyroxene, can be tested by plotting the compositions of the Eocene rocks on such graphs. Note that these graphs use cation proportions rather than weight percentages.

The test diagram for feldspar fractionation is shown in Figure 13. The Eocene pyroxene-bearing assemblage lies along a very poor trend which is nowhere close to unity and most of the samples lie considerably further from the line than the width of the correlated  $2\sigma$  error envelope. The biotite-bearing assemblage shows an even worse correlation. Even assuming that either suite is comagmatic, the chemical variation cannot be accounted for by fractionation or assimilation of feldspar alone. A similar diagram, testing for pyroxene fractionation alone, shows an absence of trends.

A better correlation is seen in Figure 14, the test diagram for fractionation of plagioclase and/or pyroxene and in the test diagram for pyroxene and feldspar (Figure 15). Samples of the pyroxene-bearing assemblage lie along recognizable trends close to a median line with a slope of 1. This suggests that chemistry in magmas of this composition is controlled dominantly by removal (or addition) of plagioclase (or feldspar) and pyroxene. The concern (J.A. Roddick, personal communication, 1996) that much of the "phenocryst" assemblage is incognate material, may be valid, but will not cause departure from the trends on this diagram.

Despite the demonstrated correlation, almost half the samples in the pyroxene-bearing assemblage lie outside the  $2\sigma$  error envelope, indicating that the suite is not related by a single chemical process. This is reasonable, considering the 5 to 8 Ma span of eruption ages. However, samples with a close spatial relationship usually lie within error of lines with a slope of 1, suggesting that this model of chemical variation can be used for specific eruptive phases or for restricted areas. Certainly, the sample containing pervasive epithermal alteration (on the far right in Figures 14 and 15) can be readily identified as the recipient of a substantial quantity of silica. This method can therefore be used in exploration, to outline areas of alteration.

One group of pyroxene-bearing samples, from the southern part of the study area, clearly lies in a field between the bulk of the pyroxene-bearing assemblage and the samples of the biotite-bearing assemblage. These lavas were either from a discrete source or have suffered contamination since generation, either by magma mixing with the biotite-bearing assemblage (unlikely given the high viscosity of silicic magmas) or by inclusion of wallrock.

Four samples from the biotite-bearing assemblage lie in a discrete trend, well within the  $2\sigma$  error envelope of a line with a slope of 2. Three samples from the suite lie off the line, one a pervasively altered sample, the second

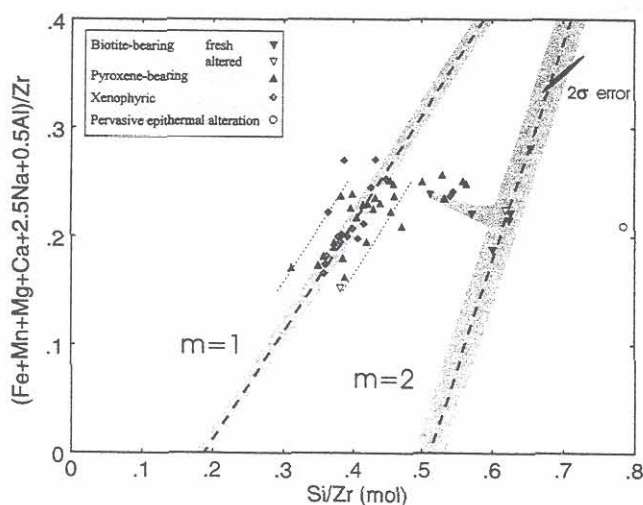


Figure 14. Pearce element ratio test diagram for plagioclase+orthopyroxene+clinopyroxene for the Clisbako volcanics. The majority of samples from the pyroxene-bearing assemblage lie within error of the unit gradient line, even those bearing xenocrysts. The 5 Ma history of the pyroxene-bearing assemblage precludes a comagmatic origin for the entire suite, but the envelope of samples lies along a slope of 1, suggesting that much of the chemical variation in the assemblage can be accounted for by fractionation of pyroxene and plagioclase. If potassium is added to the constituents (Figure 15), the grouping is tighter still. Samples from the biotite-bearing assemblage lie along a line with a slope of 2; this can be accounted for by separation of biotite and, possibly, sodic hornblende, both observed phenocryst phases in the biotite-bearing assemblage.

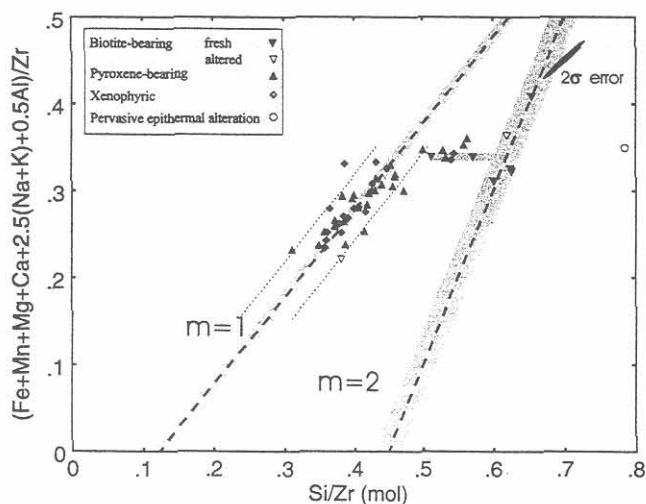


Figure 15. Pearce element ratio test diagram for feldspar+pyroxene for the Clisbako volcanics. The grouping is tighter for the pyroxene-bearing assemblage than in Figure 14, along the same trend.

(HHB94-5117) a sample with textures interpreted as the possible product of magma mixing or strong contamination. The last, from a rhyolite block in a pyroclastic flow, lies closest to the line and may have suffered minor physical contamination by pyroxene-bearing material during deposition. The slope of the line indicates that the biotite-bearing assemblage, while probably comagmatic, fails the test of pyroxene-plagioclase fractionation. The approximate slope of 2 may be coincidental; phases which would cause this trend are olivine (including fayalite), and possibly sodic biotite or hornblende. Iron titanium oxide fractionation, in conjunction with a silicate phase, could also cause this trend.

## SUMMARY

The Clisbako area is a highland area within the Chilcotin Plateau, part of the Interior Plateau of central British Columbia. This highland area is constructed from Eocene rocks, resting on a basement of Mesozoic rocks comprising Triassic fossiliferous limestone, intermediate foliated volcanic rocks of presumed Jurassic age, younger sedimentary rocks (also presumed to be Jurassic) and a clastic sedimentary sequence of Albian to Maastrichtian age. With the exception of a Triassic inlier in the east-central part of the area, faulting with centerly downthrow in the north of the area exposes younger basement to the east.

The Eocene rocks are relatively undeformed and rest on a Late Cretaceous to Paleocene erosional surface. The base of the Eocene succession is not well exposed. The erosional surface is overlain by Chilcotin Group basaltic lava flows containing olivine, plagioclase and augite phenocrysts. The flows till paleovalleys to a depth of at least 250 metres in places.

The Eocene outcrop forms a circular highland area approximately 50 kilometres across. Most of this area is underlain by a sequence of pyroxene-plagioclase-porphyrific dacite lava flows and related flowbreccias. The large volume of volcanic material and the proximal nature of the dacitic flows strongly suggest that the area is a remnant of a large volcano.

A recessive but widespread volcanic assemblage, comprising flowdomes and pyroclastic flows of biotite-bearing rhyolite, is exposed in the centre and southeastern parts of the area. This unit returned ages of 53.4 Ma to 50.9 Ma and is interpreted as the product of one or two large, caldera-forming phases of activity which destroyed the main part of the volcano. The isotopic ages are the oldest returned from the area, but the abundance of accidental fragments of pyroxene-bearing dacite in the biotite-bearing pyroclastic rocks indicates that a great volume of dacitic volcanic rock predates the rhyolitic eruption.

The biotite-bearing pyroclastic rocks are associated with a discontinuous sequence of clastic sedimentary and chemical sedimentary rocks, containing detrital biotite and also fossil flora consistent with a Middle Eocene age. These

deposits are interpreted as a caldera-filling moat facies, including deposits from hot springs. During or after this time, local hydraulic brecciation and locally intense epithermal alteration and mineralization took place, localized along northwesterly and westerly structural lineaments in the underlying basement.

A return to dacitic volcanism occurred after the pyroclastic phase and continued until at least 44 Ma; there is no field evidence for the persistence or recurrence of the pyroclastic phase of eruption. A sample from a small dome in the centre of the area returned the youngest age of all (44.2 Ma). The presence of such late domes and the moat facies is inconsistent with previous interpretations of deep erosion of the edifice. The subdued topography is probably due to a combination of central subsidence during the Eocene and inundation by basaltic lavas during and after the Miocene.

The biotite rhyolites and pyroxene-bearing lava flows are high-potassium calcalkaline lavas typical of the Ootsa Lake Group, with affinities to volcanic arc granites. Both assemblages contain plagioclase with intensely corroded cores and relict amphibole-plagioclase glomerocrysts, interpreted as incognate material, possibly from incomplete melting of the source. The major element compositions are similar to other Eocene volcanic rocks from the Interior Plateau but are distinct in their concentrations of incompatible trace elements, interpreted as further evidence for their origin from a discrete volcanic centre. The pyroxene-bearing assemblage, however, fails a Pearce element ratio test for pyroxene and plagioclase fractionation or assimilation; the duration of this type of volcanism precludes derivation from a single batch of magma. The biotite-bearing assemblage also fails this test, but both assemblages lie along discrete linear trends, which are predictable base compositions for local lithochemical exploration.

Locally intense epithermal alteration and mineralization affects rocks of the Eocene Clisbako volcanic assemblage, close to areas underlain by biotite-bearing rocks. A distinctive and similar lithological sequence is also associated with mineralization at Blackdome mine (Church, 1980, 1982), and rocks of similar age and composition host the epithermal mineralization at the nearby Wolf property (Andrew, 1988; Diakow and Webster, 1994). Biotite-bearing granitoid rocks are prospective for porphyry-related mineralization throughout the Babine and Nanika porphyry belts (Carter, 1976; Carson *et al.*, 1976; Carson and Jambor, 1976). The rocks formed from Eocene biotite-bearing magmas in the Interior Plateau, whether extrusive or intrusive, have proved highly prospective in the past and should be assigned a concomitant high potential in future exploration.

## ACKNOWLEDGMENTS

Fieldwork for this project was made possible through the British Columbia - Canada Agreement on Mineral

Development (1991-1995). The authors thank Jim Dawson of '88 Resources Ltd. and Dave Heberlein, lately of Metall Inc. (now Inmet Mining Corporation), for providing extremely useful geological information, discussions, base maps and photographs; and Peter Fox, Rob Cameron and Jeff Goodall of Fox Geological Consultants for their professional courtesy. David Bridge, lately of the Mineral Deposits Research Unit at the University of British Columbia and Adrienne Hanly, lately of Brandon University, provided invaluable assistance in the field. The B.C. Forest Service offices at Alexis Creek and Quesnel were generous in providing logistical support. Our thanks go also to Rachael Madsen for her work on the final compilation of the manuscript.

This study is based on a great deal of prior work in the Interior Plateau, particularly the landmark 1:250 000 mapping of Howard Tipper, who was also generous with his help and advice throughout the project. The contributions of Karl Schimann, Ron Bilquist, Rob Reding and Pierre Chevalier to the regional map are gratefully acknowledged. Jim Roddick's critical review of the manuscript and his helpful comments regarding incomplete melting textures in silicic rocks were greatly appreciated.

In Ottawa, we thank Fred Quigg for his technical assistance, particularly for his determination in formulating the laser/VG3600. Chris Roddick's initiative, insight and ideas are primarily responsible for the successful installation of the laser argon system; his massive contribution is not forgotten.

## REFERENCES

- Alldrick, D.J. (1989): Volcanic Centres in the Stewart Complex (103P AND 104A, B); in *Geological Fieldwork 1988, B.C. Ministry of Energy, Mines and Petroleum Resources*, Paper 1989-1, pages 233-240.
- Andrew, K.P.E. (1988): Geology and Genesis of the Wolf Precious Metal Epithermal Prospect and the Capoose Base and Precious Metal Porphyry-style Prospect, Capoose Lake Area, Central British Columbia; unpublished M.Sc. thesis, *University of British Columbia*, 300 pages.
- Carter, N.C. (1976): Regional Setting of Porphyry Deposits in West-central British Columbia; in: *Porphyry Deposits of the Canadian Cordillera*, Sutherland Brown, A., Editor, *Canadian Institute of Mining and Metallurgy*, Special Volume 15, pages 227-238.
- Carson, D.J.T. and Jambor, J.L. (1976): Morrison: Geology and Evolution of a Bisected Annular Porphyry Copper Deposit; in: *Porphyry Deposits of the Canadian Cordillera*, Sutherland Brown, A., Editor, *Canadian Institute of Mining and Metallurgy*, Special Volume 15, pages 264-273.
- Carson, D.J.T., Jambor, J.L., Ogryzlo, P. and Richards, T.A. (1976): Bell Copper: Geology, Geochemistry and Genesis of a Supergene-enriched, Biotitized Porphyry Copper Deposit with a Superimposed Phyllic Zone; in: *Porphyry deposits of the Canadian Cordillera*, Sutherland Brown, A.,

- Editor, *Canadian Institute of Mining and Metallurgy*, Special Volume 15, pages 245-263.
- Church, B.N. (1980): Exploration for Gold in the Black Dome Mountain Area (92O/7E, 8E); in *Geological Fieldwork 1979*, B.C. Ministry of Energy, Mines and Petroleum Resources, Paper 1980-1, pages 52-54.
- Church, B.N. (1982): The Black Dome Mountain Gold-Silver Prospect (92O/7E, 8W); in *Geological Fieldwork 1981*, B.C. Ministry of Energy, Mines and Petroleum Resources, Paper 1982-1, pages 106-108.
- Cook, S.J. (1993): Preliminary Report on Lake Sediment Studies in the Northern Interior Plateau, Central British Columbia (93C, E, F, K, L); in *Geological Fieldwork 1992*, Grant, B. and Newell, J.M. Editors, B.C. Ministry of Energy, Mines and Petroleum Resources, Paper 1993-1, pages 475-481.
- Cook, S.J. (1995): Gold Distribution in Lake Sediments near Epithermal Gold Occurrences in the Interior Plateau, British Columbia; in *Drift Exploration in the Canadian Cordillera*, Bobrowsky, P.T., Sibbick, S.J., Newell, J.M. and Matysek, P.F., Editors, B.C. Ministry of Energy, Mines and Petroleum Resources, Paper 1995-2, pages 193-213.
- Diakow, L.J. and Webster, I.C.L. (1994): Geology of the Fawnie Creek Map Area (93F/3); in *Geological Fieldwork 1993*, Grant, B. and Newell, J.M., Editors, B.C. Ministry of Energy, Mines and Petroleum Resources, Paper 1994-1, pages 15-26.
- Diakow, L.J., Green, K., Whittles, J. and Perry, A. (1993): Geology of the Natakuz Lake Area, Central British Columbia (NTS 93F/6); B.C. Ministry of Energy, Mines and Petroleum Resources, Open File 1993-14.
- Drobe, J.R. (1991): Petrology and Petrogenesis of the Ootsa Lake Group in the Whitesail Range, West-central British Columbia; unpublished M.Sc. thesis, *Queen's University*, 200 pages.
- Fisher, R.V. (1961): Proposed Classification of Volcanoclastic Sediments and Rocks; *Geological Society of America*, Bulletin 72, pages 1409-1414.
- Geological Survey of Canada (1994): High Resolution Aeromagnetic Total Field Survey of the Interior Plateau, British Columbia; *Geological Survey of Canada*, Open File 2785.
- Green, K.C. (1990): Structure, Stratigraphy and Alteration of Cretaceous and Tertiary Strata in the Gang Ranch Area, British Columbia; unpublished M.Sc. thesis, *University of Calgary*.
- Green, K. and Diakow, L.J. (1993): The Fawnie Range Project: Geology of the Natakuz Lake Map Area (93F/6); in *Geological Fieldwork 1992*, Grant, B. and Newell, J.M., Editors, B.C. Ministry of Energy, Mines and Petroleum Resources, Paper 1993-1, pages 57-67.
- Hickson, C.J. (1992): An Update on the Chilcotin-Nechako Project and Mapping in the Taseko Lakes Area, West-central British Columbia; in *Current Research, Part A; Geological Survey of Canada*, Paper 92-1A, pages 129-135.
- Hickson, C.J. (1993): Geology of the Northwest Quadrant, Taseko Lakes Map Area (92O), West-central British Columbia; *Geological Survey of Canada*, Open File 2695, 1:50 000 scale.
- Hickson, C.J. and Higman, S. (1993): Geology of the Northwest Quadrant, Taseko Lakes Map Area, West-central British Columbia; in *Current Research, Part A; Geological Survey of Canada*, Paper 93-1A, pages 63-67.
- Hickson, C.J., Read, P., Mathews, W.H., Hunt, J.A., Johansson, G., and Rouse, G.E. (1991): Revised Geological Mapping of Northeastern Taseko Lakes Map Area, British Columbia; in *Current Research, Part A; Geological Survey of Canada*, Paper 91-1A, pages 207-217.
- Hunt, J.A. (1992): Stratigraphy, Maturation and Source Rock Potential of Cretaceous Strata in the Chilcotin-Nechako Region of British Columbia; unpublished M.Sc. thesis, *University of British Columbia*, 448 pages.
- Irvine, T.N. and Baragar, W.R.A. (1971): A Guide to the Chemical Classification of the Common Volcanic Rocks; *Canadian Journal of Earth Sciences*, Volume 8, pages 523-548.
- LeMaitre, R.W. (1989): A Classification of Igneous Rocks and Glossary of Terms, *Blackwell Oxford*, 193 pages.
- Mathews, W.H. (1989): Neogene Chilcotin Basalts in South-central British Columbia: Geology, Ages and Geomorphic History; *Canadian Journal of Earth Sciences*, Volume 26, pages 969-982.
- Mathews, W.H. and Rouse, G.E. (1984): The Gang Ranch - Big Bar Area, South-central British Columbia: Stratigraphy, Geochronology, and Palynology of the Tertiary Beds and Their Relationship to the Fraser Fault; *Canadian Journal of Earth Sciences*, Volume 21, pages 1132-1144.
- Metcalf, P. and Hickson, C.J. (1994): Preliminary Study of Tertiary Volcanic Stratigraphy in the Clisbako River Area, Central British Columbia; in *Current Research, Part A; Geological Survey of Canada*, Paper 1994A, pages 105-108.
- Metcalf, P. and Hickson, C.J. (1995): Tertiary Volcanic Stratigraphy of the Clisbako River Area, Central British Columbia; in *Current Research, Part A; Geological Survey of Canada*, Paper 1995A, pages 67-73.
- Pearce, J.A., Harris, N.B.W. and Tindle, A.G. (1984): Trace Element Discrimination Diagrams for the Tectonic Interpretation of Granitic Rocks; *Journal of Petrology*, Volume 25, pages 956-983.
- Piel, K. (1971): Palynology of Oligocene Sediments From Central British Columbia; *Canadian Journal of Botany*, Volume 49, pages 1885-1920.
- Proudfoot, D.N. (1993): Drift Exploration and Surficial Geology of the Clusko River and Toil Mountain Map Sheets (93C/19,16); in *Geological Fieldwork 1992*, Grant, B. and Newell, J.M., Editors, *British Columbia Ministry of Energy, Mines and Petroleum Resources*, Paper 1993-1, pages 491-498.
- Renne, P.R., Deino, A.L., Walter, R.C., Turrin, B.D., Swisher, C.C., Becker, T.A., Curtis, G.H., Sharp, W.D. and Jaouni, A.-R. (1994): Intercalibration of Astronomical and Radiometric time, *Geology*, Volume 22, pages 783-786.
- Ridgway, K.D., Sweet, A.R. and Cameron, A.R. (1995): Climatically Induced Floristic Changes Across the Eocene-Oligocene Transition in the Northern Latitudes, Yukon Territory, Canada; *Geological Society of America*, Bulletin, Volume 107, pages 676-696.

- Roddick, J.C. (1988): The Assessment of Errors in  $^{40}\text{Ar}/^{39}\text{Ar}$  Dating; in Radiogenic Age and Isotopic Studies: Report 2, *Geological Survey of Canada*, Paper 88-2, pages 7-16.
- Roddick, J.C. (1990):  $^{40}\text{Ar}/^{39}\text{Ar}$  Evidence for the age of the New Quebec Crater, Northern Quebec; in Radiogenic Age and Isotopic Studies: Report 3, *Geological Survey of Canada*, Paper 89-2, pages 7-16.
- Roddick, J.C. (1995): Efficient Mass Calibration of Magnetic Sector Mass Spectrometers; in Radiogenic Age and Isotopic Studies: Report 9, *Geological Survey of Canada*, Paper 1995-F, pages 1-9.
- Roddick, J.C., Cliff, R.A. and Rex, D.C. (1980): The Evolution of Excess Argon in Alpine Biotites — A  $^{40}\text{Ar}/^{39}\text{Ar}$  analysis; *Earth and Planetary Science Letters*, Volume 48, pages 185-208.
- Rouse, G.E. and Mathews, W.H. (1979): Tertiary Geology and Palynology of the Quesnel Area, British Columbia; *Bulletin of Canadian Petroleum Geology*, Volume 27, pages 418-445.
- Rouse, G.E. and Mathews, W.H. (1988): Palynology and Geochronology of Eocene Beds from Cheslatta Falls and Nazko Areas, Central British Columbia; *Canadian Journal of Earth Sciences*, Volume 25, pages 1268-1276.
- Russell, J.K. and Nicholls, J. (1988): Analysis of Petrologic Hypotheses with Pearce Element Ratios; *Contributions to Mineralogy and Petrology*, Volume 99, pages 25-35.
- Russell, J.K. and Stanley, C.R.J. (1990): Matrix Methods for the Development of Pearce Element Ratio Diagrams, in Theory and Application of Pearce Element Ratios to Geochemical Data Analysis; Russell, J.K. and Stanley, C.R., Editors, *Geological Association of Canada*, Short Course Volume 8, pages 131-156.
- Shives, R.B.K. and Carson, J.M. (1994): Multiparameter Airborne Geophysical Survey of the Clisbako River Area, Interior Plateau Region, British Columbia (parts of 93B/12, 93C/9, 93C/16); *Geological Survey of Canada*, Open File 2815, 56 pages.
- Smith, A.D. (1986): Isotopic and Chemical Studies of Terrane I, South-central British Columbia; unpublished Ph.D. thesis, *University of Alberta*, 195 pages.
- Souther, J.G., Clague, J.J. and Mathews, R.W. (1987): Nazko Cone: A Quaternary Volcano in the Eastern Anahim Belt; *Canadian Journal of Earth Sciences*, Volume 18, pages 2477-2485.
- Teskey, D., Stone P., Mustard, P. and Metcalfe, P. (1996): High-resolution Regional Aeromagnetic Survey -Interior Plateau British Columbia; in *Interior Plateau Geoscience Project: Summary of Geological, Geochemical and Geophysical Studies*, Newell, J.M. and Diakow, L.J., Editors, *B.C. Ministry of Employment and Investment*, Paper 1997-2.
- Tipper, H.W. (1959): Geology, Quesnel, British Columbia (93C); *Geological Survey of Canada*, Map 12-1959, 1" to 4 miles.
- Tipper, H.W. (1969): Geology, Anahim Lake, British Columbia (93B); *Geological Survey of Canada*, Map 1202A, 1" to 4 miles.
- van der Heyden, P., Shives, R., Ballantyne B., Harris, D., Dunn, C., Teskey, D., Plouffe, A. and Hickson, C.J. (1993): Overview and Preliminary Results for the Interior Plateau Program, Canada - British Columbia Agreement on Mineral Development 1991-1995; in *Current Research, Part E, Geological Survey of Canada*, Paper 93-1E, pages 73-79.
- van der Heyden, P., Mustard, P., Metcalfe, P., Shives, R., Plouffe, A., Teskey, D., and Dunn, C. (1995): Interior Plateau Program, Canada/British Columbia Agreement on Mineral Development 1991-1995: An Update; in *Current Research Part A, Geological Survey of Canada*, Paper 1995A, pages 75-80.

